

**Optimal stochastic scheduling of plug-in electric vehicles
as mobile energy storage systems for resilience
enhancement of multi-agent multi-energy networked
microgrids**

AHMADI, Seyed Ehsan, MARZBAND, Mousa, IKPEHAI, Augustine and
ABUSORRAH, Abdullah

Available from Sheffield Hallam University Research Archive (SHURA) at:

<https://shura.shu.ac.uk/30642/>

This document is the Accepted Version [AM]

Citation:

AHMADI, Seyed Ehsan, MARZBAND, Mousa, IKPEHAI, Augustine and
ABUSORRAH, Abdullah (2022). Optimal stochastic scheduling of plug-in electric
vehicles as mobile energy storage systems for resilience enhancement of multi-
agent multi-energy networked microgrids. Journal of Energy Storage, 55 (B):
105566. [Article]

Copyright and re-use policy

See <http://shura.shu.ac.uk/information.html>

Optimal Stochastic Scheduling of Plug-in Electric Vehicles as Mobile Energy Storage Systems for Resilience Enhancement of Multi-Agent Multi-Energy Networked Microgrids

Seyed Ehsan Ahmadi^a, Mousa Marzband^{a,b}, Augustine Ikpehai^c, Abdullah Abusorrah^{b,d}

^aNorthumbria University, Electrical Power and Control Systems Research Group, Ellison Place NE1 8ST, Newcastle upon Tyne, UK

^bCenter of Research Excellence in Renewable Energy and Power Systems, King Abdulaziz University, Jeddah, 21589, Saudi Arabia

^cDepartment of Engineering and Mathematics, Sheffield Hallam University, Sheffield S1 1WB, UK

^dDepartment of Electrical and Computer Engineering, Faculty of Engineering, K. A. CARE Energy Research and Innovation Center, King Abdulaziz University, Jeddah 21589, Saudi Arabia

Abstract

This paper presents an optimal scheduling of plug-in electric vehicles (PEVs) as mobile power sources for enhancing the resilience of multi-agent systems (MAS) with networked multi-energy microgrids (MEMGs). In each MEMG, suppliers, storage, and consumers of energy carriers of power, heat, and hydrogen are taken into account under the uncertainties of intermittent nature of renewable units, power/heat demands, and parking time of PEVs. In the case of contingencies, the proposed algorithm supplies energy to the on-fault MEMGs from normal-operated grid-connected MEMGs, using mobile PEVs. The procedure of selecting PEVs to supply energy to the on-fault MEMGs is performed in three stages. Initially, both on-fault and normal-operated MEMGs inform the central energy management system (EMS) about the amount of required energy and the amount of available energy from existing PEVs. Further, central EMS prioritizes the MEMGs among networked MEMGs to supply the energy support to the on-fault islanded MEMG. Lastly, the chosen MEMGs select their available efficient PEVs to supply energy to the on-fault islanded MEMG.

Email address: mousa.marzband@northumbria.ac.uk Corresponding author (Mousa Marzband)

Considering two diverse faulty case studies, the proposed technique is investigated in a MAS with four networked MEMGs. Simulated results demonstrate that the proposed algorithm enhances the resilience of MEMGs (over 25%) even without a physical connection between the MEMGs.

Keywords: Resilience enhancement, hierarchical energy management, multi-agent system, multi-energy microgrids, electric vehicle.

Nomenclature

Acronyms

BES	Battery Energy Storage
CHP	Combined Heat and Power
DER	Distributed Energy Resource
DG	Distribution Generator
DS	Distribution System
EMS	Energy Management System
ESS	Energy Storage System
H2P	Hydrogen to Power
HES	Hydrogen Energy Storage
MAS	Multi-Agent System
MEG	Mobile Emergency Generators
MEMG	Mobile Emergency Generators
MPS	Mobile Power Source
MT	Micro Turbine
P2H	Power to Hydrogen
PEV	Plug-in Electric Vehicle
PL	Parking Lot
PV	Photovoltaic

SoC	State of Charge
TES	Thermal Energy Storage
V2G	Vehicle to Grid
WT	Wind Turbine

Indices

m	Index for microgrids
i	Index for nodes
g	Index for MTs
c	Index for CHP units
e	Index for renewable units
b	Index for BESs
v	Index for PEVs
h	Index for HESs
t	Index for scheduling time
s	Index for scenarios

Sets

I_m, I'_m	Set of loads in normal-operated/ on-fault MEMG m
G_m, G'_m	Set of MTs in normal-operated/ on-fault MEMG m
C_m, C'_m	Set of CHP units in normal-operated/ on-fault MEMG m
E_m, E'_m	Set of RESs in normal-operated/ on-fault MEMG m
B_m, B'_m	Set of BESs in normal-operated/ on-fault MEMG m
V_m, V'_m	Set of PEVs in normal-operated/ on-fault MEMG m
H_m, H'_m	Set of HESs in normal-operated/ on-fault MEMG m
M_N, M_F	Set of normal-operated/ on-fault MEMGs
T	Set of scheduling time horizon
S	Set for scenarios

Parameters

$P_g^{MT,min}, P_g^{MT,max}$	Minimum/ maximum allowable power generation of MT g (kW)
$P_g^{MT,RU}, P_g^{MT,RD}$	Active ramp up/ down boundaries of MT g (kW)
$P_c^{CHP,min}$	Minimum allowable power generation of CHP unit c (kW)
$P_c^{CHP,RU}, P_c^{CHP,RD}$	Power ramp up/ down boundaries of CHP unit c (kW)
UT_j^{CHP}, DT_j^{CHP}	Minimum up/ down time of CHP units (hr)
$P_{i,t,s}^{Load}$	Power demand at node i at hour t for scenario s (kW)
$H_{i,t,s}^{Load}$	Heat demand at node i at hour t for scenario s (kWt)
$E_h^{HES,min}, E_h^{HES,max}$	Minimum/ maximum capacity of HES h (kW)
$P_h^{P2H,min}, P_h^{P2H,max}$	Minimum/ maximum convertible power to hydrogen in HES h (kW)
$P_h^{H2P,min}, P_h^{H2P,max}$	Minimum/ maximum convertible hydrogen to power in HES h (kW)
$SOC_b^{BES,min}, SOC_b^{BES,max}$	Minimum/ maximum state of charge of BES b (%)
$P_b^{BES,Cap}$	Maximum capacity of storing energy in BES b (kW)
$E^{PEV,Res}$	Energy reserved for resilience in the PEV batteries parked at PLs (kW)
$SOC_v^{PEV,min}, SOC_v^{PEV,max}$	Minimum/ maximum PEV battery v state of charge (%)
$SOC_v^{PEV,Dep}$	State of charge of PEV battery v in departure time (%)
$P_v^{PEV,Cap}$	Maximum capacity of storing energy in PEV battery v (kW)
$N_{m,t,s}^{PEV,Parked}$	Number of PEVs parked in PLs in MEMG m at hour t for scenario s
$\underline{E}_{(v)}^{PEV}, \bar{E}_{(v)}^{PEV}$	Minimum/ maximum level of stored power in PEV v (MW)
$P_{e,t,s}^{WT}$	WT e power generation at hour t for scenario s (kW)
$P_{e,t,s}^{PV}$	PV e power generation at hour t for scenario s (kW)
$\alpha_g^{MT,1}, \alpha_g^{MT,2}$	Cost parameters of MT g
$\phi_c^{CHP,1}, \phi_c^{CHP,3}$	Cost coefficients of power generation in CHP unit c
$\psi_c^{CHP,1}, \psi_c^{CHP,3}$	Cost coefficients of heat generation in CHP unit c
PA_c^{CHP}, PD_c^{CHP}	Operation regions of power generation in CHP unit c (kW)
HA_c^{CHP}, HD_c^{CHP}	Operation regions of heat generation in CHP unit c (kWt)
$\eta^{BES,ch}, \eta^{BES,dch}$	Charge/ discharge efficiency of BESs (%)
$\eta^{PEV,ch}, \eta^{PEV,dch}$	Charge/ discharge efficiency of PEV batteries (%)

η^{P2H}, η^{H2P}	Charging/ discharging efficiency of HESs (%)
$E f_v^{PEV}$	Energy consumption efficiency of PEV v (W/km)
μ_t^{GS}	Price of selling power to the utility grid at hour t (\$/MWh)
μ_t^{GB}	Price of buying power from the utility grid at hour t (\$/MWh)
μ_t^{BES}	Charging price of BESs at hour t (\$/kWh)
$\mu_t^{Hyd, Char}$	Charging price of HESs at hour t (\$/kWh)
μ_t^{PEV}	Charging price of PEV batteries at hour t (\$/kWh)
γ_s	Scenario s probability [0-1]
Z	An adequately large number

Variables

$P_{g,t,s}^{MT}$	Power generation of MT g at hour t for scenario s (kW)
$P_{c,t,s}^{CHP}, H_{c,t,s}^{CHP}$	Power/ Heat generation of CHP unit c at hour t for scenario s (kW/kWt)
$P_{h,t,s}^{P2H}, P_{c,t,s}^{H2P}$	Charging/ discharging amount of HES h at hour t for scenario s (kW)
$E_{h,t,s}^{HES}$	Energy level of HES h at hour t for scenario s (kW)
$P_{v,t,s}^{PEV, ch}, P_{v,t,s}^{PEV, dch}$	Charged/ discharged power of PEV battery v at hour t for scenario s (kW)
$SOC_{v,t,s}^{PEV}$	PEV battery v state of charge at hour t for scenario s (%)
$E_{m \rightarrow n,t,s}^{PEV, Sup}$	Energy supplied by MEMG m to MEMG n at hour t for scenario s (kW)
$E_{m \rightarrow n,t,s}^{Available}$	Available energy stored in batteries of agreed PEVs in MEMG m (kW)
$E_{v,t,s}^{PEV, Store}$	Energy stored in PEV v at hour t for scenario s (kW)
$E_{v,t,s}^{PEV, Parked}$	Energy stored in batteries of PEVs in MEMG m (kW)
$J_{m \rightarrow n}^{Dis}$	Information of distance between MEMG m and MEMG n (km)
$D_{m \rightarrow n}$	Distance between MEMG m and MEMG n (km)
D^{Max}	Maximum distance between networked MEMGs (km)
$v_{v,t,s}^{Agree}$	Participation status of PEV owner v at hour t for scenario s [0,1]
$\omega_{m,t,s}^{Agree}$	Participation factor of PEV owners to supply power [0,1]
$P_{b,t,s}^{BES, ch}, P_{b,t,s}^{BES, dch}$	Charged/ discharged power of BES b at hour t for scenario s (kW)
$SOC_{b,t,s}^{BES}$	State of charge of BES b at hour t for scenario s (%)
$P_{m,t,s}^{Sur}$	Surplus power in MEMG m at hour t for scenario s (kW)
$P_{m,t,s}^{Short}$	Shortage power in MEMG m at hour t for scenario s (kW)

$P_{m,t,s}^{EX}$	Power exchange in MEMG m at hour t for scenario s (kW)
$P_{m,t,s}^{GB}$	Power bought from the utility grid in MEMG m at hour t for scenario s (kW)
$P_{m,t,s}^{GS}$	Power sold to the utility grid in MEMG m at hour t for scenario s (kW)
$P_{m \rightarrow n,t,s}^{Send}$	Power sent from MEMG m to MEMG n at hour t for scenario s (kW)
$P_{m \leftarrow n,t,s}^{Rec}$	Power received from MEMG n to MEMG m at hour t for scenario s (kW)
$P_{n,t,s}^{Def}$	Power deficiency in on-fault islanded MEMG n at hour t for scenario s (kW)
$P_{n,t,s}^{Shed}$	Load shedding in on-fault islanded MEMG n at hour t for scenario s (kW)
$\mathcal{C}_{m,t,s}^{MT}$	MT cost function in MEMG m (\$)
$\mathcal{C}_{m,t,s}^{CHP}$	CHP unit cost function in MEMG m (\$)
$\mathcal{C}_{m,t,s}^{BES}$	BES charging cost function in MEMG m (\$)
$\mathcal{C}_{m,t,s}^{PEV}$	PEV charging cost function in MEMG m (\$)
$\mathcal{C}_{m,t,s}^{HES}$	HES charging cost function in MEMG m (\$)
$\mathcal{R}_{m,t,s}^{Sur}$	Revenue function of surplus electrical power in MEMG m (\$)
$\mathcal{C}_{m,t,s}^{Short}$	Cost function of shortage electrical power in MEMG m (\$)
$Cost_m$	Total operation cost of MEMG m in normal operation mode (\$)
$\sigma_{g,t,s}^{MT, UC}$	Status of MT g at hour t for scenario s [0,1]
$\sigma_{g,t,s}^{SU}, \sigma_{g,t,s}^{SD}$	Start-up/ shut-down state of MT g at hour t for scenario s [0,1]
$\sigma_{c,t,s}^{CHP, UC}$	Status of CHP unit c at hour t for scenario s [0,1]
$\sigma_{c,t,s}^{CHP, SU}, \sigma_{c,t,s}^{CHP, SD}$	Start-up/ shut-down state of CHP unit c at hour t for scenario s [0,1]
$\sigma_{h,t,s}^{P2H}, \sigma_{h,t,s}^{H2P}$	Charge/ discharge state of HES h at hour t for scenario s [0,1]
$\sigma_{b,t,s}^{PEV, ch}, \sigma_{b,t,s}^{PEV, dch}$	Charge/ discharge state of BES b at hour t for scenario s [0,1]
$\sigma_{v,t,s}^{PEV, ch}, \sigma_{v,t,s}^{PEV, dch}$	Charge/ discharge state of PEV battery v at hour t for scenario s [0,1]
$\sigma_{m,t,s}^{Sur}, \sigma_{m,t,s}^{Short}$	Surplus/ shortage power state of MEMG m at hour t for scenario s [0,1]

1. Introduction

1.1. Motivations

About 70% of power outages are because of contingencies in distribution systems (DSs) [1]. Disaster disruptions can result in multiple line outages in DSs, thus, jeopardizing the security and permanence of customer service. Consequently, preventive measures are necessary to enhance DS resilience to against extreme events, by utilising available resources in a further proactive and cooperative approach to realize faster power support and restoration [2, 3]. Diverse strategies have been proposed for enhancing the resilience of the system, and the most commonly used ones among them are the incorporation of distributed energy resources (DERs), microgrid formation, and power line hardening [4]. Generally, the DS resilience can be enhanced in three main stages: (1) planning stage, (2) response stage, and (3) restoration stage. The response stage may be assorted into the preventive and emergency response stages [5]. Figure 1 shows the assortment and functional objectives of each stage. In the planning stage, the preventive actions on vital power assets can enhance the system robustness and resource accessibility. In the preventive response stage, emergency power resources is pre-allocated, and preventive scheduling strategies can be adapted in preparation for the forthcoming extreme events. In the emergency response stage, priority loads is restored via the real-time flexible methods in accordance with the available resources. In the restoration stage, the maintenance crews are sent to repair the impaired facilities, therefore the DS is returned to the normal operation mode step by step [6–8].

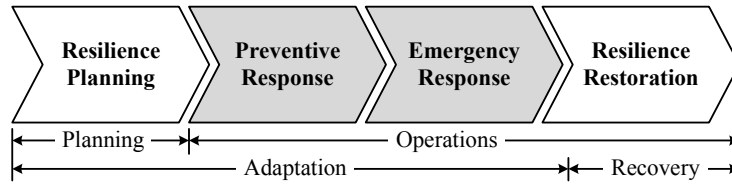


Figure 1: Resilience enhancement stages

In recent years, microgrid design techniques for power generation have widely been discussed, but there is limited research on the performance of multi-energy

microgrids (MEMGs) for resilience enhancement. Based on the increased difficulty of multiple possible combinations between energy vectors and technologies, this is a particularly demanding research topic. Distributed generators (DGs) such as combined heat and power (CHP) units and micro-turbines (MTs), renewable energy resources (RESs), vehicle-to-grid (V2G), power to hydrogen (P2H) and hydrogen to power (H2P) facilities, diverse types of energy storage systems (ESSs) such as stationary and mobile battery energy storages (BESs), thermal energy storages (TESs), and hydrogen energy storages (HESs) are standard resources in MEMGs [9]. MEMGs are one of the effective frameworks for enhancing the resilience of the system, reducing energy costs, and decreasing CO₂ and greenhouse emissions [10, 11]. Mobile power sources (MPSs), consisting of plug-in electric vehicles (PEV), mobile energy storage systems (MESSs), and mobile emergency generators (MEGs), can be taken into account as the flexible sources to enhance the resilience of DSs [7, 12]. In comparison with other resilience response strategies, the MESSs have various advantages. They are more eco-friendly than MEGs and can be utilized without redundant noise and air pollution. Furthermore, different from preventive load shedding or adaptive microgrids, the MESSs can be promptly scheduled by the network operator in such a way that the progressive communication framework is not needed [13, 14]. On the other hand, due to decrease in manufacturing cost, advanced technologies of batteries, and their environmental advantages, PEVs are growing day by day and play an important role in enhancing the resilience of MEMGs. Also, the saved energy in a PEV can be delivered to the grid in parking lots (PLs) as a V2G facility [15].

Resilience enhancement schedules of microgrids attain popularity because of their capability to sustain the penetration of RESs and resist disturbances in the islanded mode. Furthermore, the DS resilience can be enhanced by transforming it into several microgrids or by developing networked microgrids as a single aggregated entity for service restoration to priority loads [16]. Furthermore, microgrids include diverse DERs and customers, which can be modeled as autonomous agents. Each agent subject to its type and configuration, has a specific intelligence level to seek planned objectives. Since multi-agent system (MAS) idea is thoroughly as-

sociated with distributed intelligence, it is an appropriate prospect to establish an intelligent energy management system (EMS) in microgrids [17, 18]. [In order to implement a proper EMS for MAS-based networked MEMGs, the hierarchical method is investigated in this paper.](#) The hierarchical energy management approach relies on local distributed EMS located in each MEMG. These local EMSs can intercommunicate to realize the objectives subject to a given hierarchical algorithm. Furthermore, the hierarchical energy management approach offers an accurate energy flow between networked MEMGs, allowing a MEMG to exchange the surplus/shortage energy with other MEMGs for a paid charge to enhance the system's resiliency [19, 20]. Accordingly, based on the predefined uncertainties and energy balance constraints, a hierarchical energy management approach is proposed for enhancing the resilience of a MAS with networked MEMGs using existing PEVs.

1.2. [Literature Review](#)

In recent years, the resilience enhancement strategies have been studied in the literature, but the MESSs have not been investigated in a MAS with networked MEMGs. In [21], a stochastic nonlinear framework is presented for the optimal energy management of the unbalanced three-phase AC microgrids. Furthermore, the suggested model aims to provide resilient energy management solutions via contingency constraints. In [22], a linear optimization framework is proposed for optimal locating of sectionalizing switches and backup DGs to enhance the resilience of the system under extreme events. In the suggested framework, low priority, medium priority and high priority loads are taken into account and a demand response program is also applied on a modified IEEE 33-bus DS. In [23], a new two-level stochastic planning scheme is presented for enhancing the resilience of DSs. The first level is to decide on line hardening, DG and MEG allocation, and placement of tie switches, while the second level is to minimize the operating costs of power purchase from the utility grid, DGs, and emergency load shedding in extreme events. Although the planning stage has considered enhancing the network's resilience in [21–23], the MPSs are not taken into account. Authors in [24] have presented a restoration strategy taking into account the wind power cut-off for enhancing the

resilience of the modified IEEE-69 distribution system. The resilient enhancement strategy takes advantage of MESSs, repair crews, network reconfiguration, and DGs to restore the on-fault DS. In [25], an MILP framework is proposed to restore priority loads while satisfying topology and operating constraints to enhance resilience of the DS under extreme events. In the presented framework, dynamic microgrid formation and optimal management of diverse smart technologies are taken into account as well as the required emergency operating budgets. Although the planning stage and the corresponding uncertainties of renewable energies and loads have considered for enhancing the network's resilience in [24] and [25], the MPSs are not taken into account.

In [26], a comprehensive resilience enhancement strategy is presented for multi-energy systems using the multi-stage recovery procedure for enhancing the system ability withstand and recover rapidly from an extreme event. Several resilience enhancement measures are adopted, and their coupling relationships at diverse stages are also considered. In [27], a coordinated regional-district scheduling of an integrated energy system is proposed as an energy hub to enhance resilience in extreme events. Furthermore, a tri-level robust algorithm is presented to coordinate random fault scenarios in natural gas and electricity generation and delivery systems. However, in [26] and [27], a deterministic framework has been utilized for energy management and the implementation of MPSs has been neglected. In [28], a stochastic programming model is proposed for enhancing the resilience of DSs to handle extreme events. The suggested model considers the traveling time of crew teams to the manual switches sites in the transportation structure. Besides, the crews and MEGs are pre-positioned in staging location. In [29], the configuration of adaptive multi-microgrids is proposed as the critical service restoration method. The suggested strategy includes load switching sequence steps, the configuration of multi-microgrids, and optimal allocation of MEGs. Although, the MPSs have taken into account in the planning stage of resiliency in [28] and [29], a deterministic framework has been proposed for energy management. In [30], a bi-level optimization strategy is presented for enhancing the resilience of DSs, which is convinced by a transportation system. The first level is to pre-position the emergency

stations and the second level is to co-optimize the dispatch of MESSs and repair crews on the transportation system to minimize the emergency load shedding. In [31], resilience enhancement of the DSs against earthquakes is presented by taking into account road traffic and interruption time as the main issues applying the MESSs. To better realize the performances, BES and MESS are compared under the same conditions. The results indicated that the MESSs are 62% more resilient than BESs due to the mobility nature of MESSs. In [32], a bi-level optimization strategy is presented to optimise investments in MESSs in the first level and re-routes the installed MESSs in the second level to develop dynamic microgrids and to prevent the expected load shedding triggered by extreme events. Although, the utilization of MPSs have been proposed in the operation stage of resiliency in [30–32], a deterministic framework has been considered for the scheduling problem.

In [33], a restoration method is developed in DSs for routing, and scheduling of MESSs integrated with indeterminate nature of RESs to attain rapid system response and recovery against the consequences of high-impact low-probability extreme events. Authors in [34] have demonstrated the effects of MESSs and diesel DGs in the integrated electrical-heating systems to enhance resilience and decrease load shedding and operating costs. Two fault scenarios are generated in the electricity and natural to investigate the resilience and load restoration measures. In [35], a tri-level multi-objective short-term resilience enhancement strategy is proposed for the multiple residential energy systems such as integrated gas, heat and electrical against hurricane at day-ahead. The lines outage in the electrical DS is applied as a stochastic model including installation of MEGs, demand side management strategy, and local generation in each level. Although, the MPSs have been considered in the operation stage of resiliency in [33–35], the MAS framework and the networked structure have not been proposed for the optimization problem of microgrids. In [36], a tri-level stochastic planning strategy is presented for allocating of MEGs in resilient DSs considering different resiliency stages. The uncertainty of the given extreme events are also taken into account for the effective allocation of MEGs. Moreover, the MEGs are pre-positioned and re-routed to the defined location. However, the uncertainty analysis, the MAS-based architecture,

and the networked connection of microgrids have not been considered. In [37], a two stage algorithm is proposed for resilience enhancement of electricity-gas-heating networks considering fast-acting flexible loads, PEVs, power-to-gas technologies, and gas storage systems. In the first stage, the optimization problem is solved by a decentralized framework and in the second stage, DS operator schedules the electricity-gas-heating networks. Although the MPSs and multi-energy systems have been proposed for the operation stage of resiliency, the MAS framework and networked structure have not been considered. Authors in [38] have presented a tri-level algorithm for resolving the resilience-driven optimal allocation and pre-positioning constraints of MESSs in the networked microgrids with decentralized energy management framework. The first level is proposed for achieving optimization results opposing a certain extreme event, while the second and the third levels are integrated as a sub-problem to designate a scenario that can cause the most extreme event. Although the networked microgrids and the MPSs has been proposed for the planning stage of resiliency, the MAS has not been considered.

1.3. *Paper Scopes and Contributions*

According to the literature mentioned above regarding the resilience enhancement strategies in DSs and microgrids, it is evident that:

1. Previous works failed to consider a resilience enhancement strategy for a MAS with networked MEMGs under the system uncertainties;
2. The MAS has not been investigated to consider the autonomy of MEMGs;
3. The networked structure of MEMGs as a multi-carrier energy network has not been proposed in previous works;
4. Previous works have not taken into account the aggregation of PEVs as an autonomous agent of transportation in a MAS to properly investigated the V2G facility;
5. The uncertainty of the arrival/departure timing of PEVs has not been studied in the literature for taking into account the commuting time of PEV owners as a vital factor in optimization problems;

6. Finally, the level of participation and ability of PEV owners to compensate for power deficiency has not been studied in the previous works.

In order to fill the gap of previous works, the proposed strategy in this paper considers all the limitations noted in the above paragraphs to resolve the optimal scheduling of resiliency enhancement mode in networked MEMGs. In this study, the resilience is defined as the ability of the network to endure against any contingency owing to the support of PEVs. The MEMG contains electricity, heating, and hydrogen energy networks, coupled by a MAS framework. Based on the coupling components, different types of energy in the MEMG can be generated, stored, and consumed with direct communication among agents.

Table 1 illustrates a thorough comparison between the proposed strategy of this paper and the literature reviewed. Accordingly, in this paper, a hierarchical EMS is proposed for the stochastic optimization of a MAS with networked MEMGs (including power, heat, and hydrogen energy carriers) under the uncertainties of the RESs, power/heat loads, and parking time of PEVs in PLs. When a fault occurs in the networked MEMGs, existing PEVs in the normal-operated MEMGs can be applied for enhancing the resilience of on-fault MEMGs in the proposed hierarchical algorithm. The on-fault MEMGs need not be physically connected with the normal-operated MEMGs. Eventually, by investigating the proposed strategy, MEMGs with a few PEVs can also enhance their resilience by supplying their priority loads through PEVs of other MEMGs. To realize these aims, an optimization algorithm is suggested to schedule the required energy support to the islanded part of the on-fault MEMG (disconnected from the network as a consequence of any contingency) from the grid-connected normal-operated MEMGs in the networked structure applying PEVs. PEVs from the normal-operated MEMG travel to the islanded part of the on-fault MEMG to supply energy. Besides, the level of participation of PEV owners to compensate for power deficiency in an on-fault network is also taken into account in the optimization problem. The proposed model is optimized over a MAS with four MEMGs in three diverse case studies, including normal operation case, a case with one fault, and case with two simultaneous faults.

Table 1: comparison between the proposed strategy and different research works on the resilience enhancement in DSs and microgrids

Reference	Uncertain Parameters			EMS			Approach Components				Resilience Stage	
	RES	Load	Parking Time	Centralized	Decentralized	Hierarchical	MAS	Networked Structure	Multi Energy Carrier	MPSS	Planning	Operation
[21]	✓	✓	✗	✓	✗	✗	✗	✗	✗	✗	✓	✗
[22]	✗	✓	✗	✓	✗	✗	✗	✗	✗	✗	✓	✗
[23]	✗	✓	✗	✓	✗	✗	✗	✗	✓	✗	✓	✗
[24]	✓	✓	✗	✓	✗	✗	✗	✗	✗	✗	✗	✓
[25]	✓	✓	✗	✓	✗	✗	✗	✗	✗	✗	✗	✓
[26]	✗	✗	✗	✓	✗	✗	✗	✗	✓	✗	✗	✓
[27]	✗	✗	✗	✓	✗	✗	✗	✗	✓	✗	✗	✓
[28]	✗	✗	✗	✓	✗	✗	✗	✗	✗	✓	✓	✗
[29]	✗	✗	✗	✓	✗	✗	✗	✗	✗	✓	✓	✗
[30]	✗	✗	✗	✓	✗	✗	✗	✗	✗	✓	✗	✓
[31]	✗	✗	✗	✓	✗	✗	✗	✗	✗	✓	✗	✓
[32]	✗	✗	✗	✓	✗	✗	✗	✗	✗	✓	✗	✓
[33]	✓	✗	✗	✓	✗	✗	✗	✗	✗	✓	✗	✓
[34]	✓	✓	✗	✓	✗	✗	✗	✗	✓	✓	✗	✓
[35]	✗	✓	✗	✓	✗	✗	✗	✗	✓	✓	✗	✓
[36]	✗	✗	✗	✓	✗	✗	✗	✗	✗	✓	✓	✓
[37]	✓	✓	✗	✗	✓	✗	✗	✗	✓	✓	✗	✓
[38]	✓	✓	✗	✗	✓	✗	✗	✓	✗	✓	✓	✗
Proposed Model	✓	✓	✓	✗	✗	✓	✓	✓	✓	✓	✗	✓

1.4. *Paper Organization*

The rest of the paper is divided into the following sections. In Section 2, the resilience enhancement strategy for the proposed MAS-based framework of networked MEMGs is presented. *First, the system model and components of networked MEMGs is reviewed. Then the scenario-based analysis is presented to model the uncertain parameters. Last, normal operation and resilience enhancement modes are represented.* In Section 3, the mathematical modeling of the hierarchical EMS of the MAS-based networked MEMGs is indicated. Simulation results of the optimization algorithm's normal operation and resilience enhancement modes are presented in Section 4 with two diverse fault scenarios. As a conclusion, some points are highlighted in Section 5.

2. Resilience Enhancement Method for the Proposed MAS-based framework

2.1. *System Model and Components of MAS-Based Networked MEMGs*

The architecture of the proposed MAS for networked MEMGs is shown in Figure 2 and it relies on the agents that represent various entities in a MEMG. A MEMG can exchange active power with other MEMGs in the networked system and trade active power with the upstream grid. MEMGs consist of dispatchable DGs including CHP unit and MT, non-dispatchable DGs including wind turbines (WT) and photovoltaic (PV), multi-ESSs including BES and HES, PEV as the MESS, and electrical and heat loads [9]. The MAS structure for networked MEMGs is optimized systematically using local EMSs and a central EMS. In this structure, six kinds of agents can be proposed in each MEMG: electricity agent, heat agent, hydrogen agent, transportation agent, local energy management agents (LEMA), and central energy management agents (CEMA). The electricity agent represents MTs, RESs, BESs, and electrical loads, while the heat, hydrogen, and transportation agents represent CHP units and heat loads, HESs, and PEVs, respectively. Each agent can control and monitor their local energy generation and demand. Besides, each MEMG can regulate energy prices for their intercommunication with the LEMA. Accordingly, the LEMA

is the primary operator of a MEMG assuring energy balance between local consumers and their available energy suppliers, while interacts with electricity agent to optimize the total operating costs. Therefore, the local EMS performs the local optimization level of MEMGs. Then, the local EMS sends the required data to the central EMS as CEMA ensuring global optimization level of the networked MEMGs. Central EMS runs the optimization algorithm in accordance with the data perceived from local EMSs. The solution to the EMS problem decreases the MEMG operating cost while assuring the physical and technical constraints of the system.

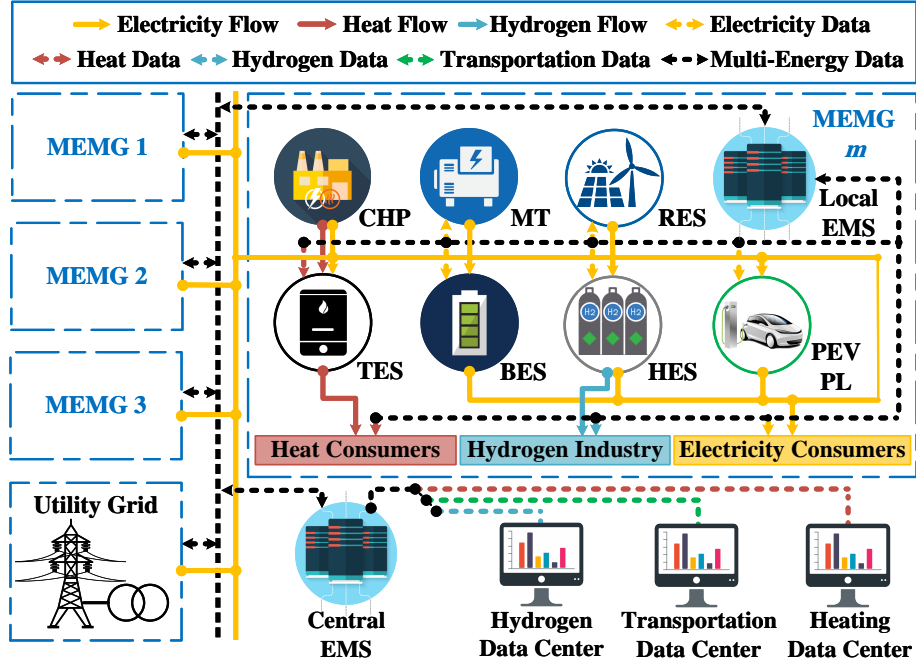


Figure 2: System model of hierarchical EMS for MAS-based networked MEMGs

2.2. Scenario-Based Analysis Modelling

Due to the stochastic nature of the renewable generations, power/heat loads, and the behavior patterns of parking time of PEVs in PLs, investigating a deterministic strategy will not ensure a deep insight into the potential benefits of integrating DERs. For adequately managing the uncertain parameters, a scenario-based analysis (SBA) is utilized to generate the diverse scenarios. Besides, a backward scenario

reduction method is proposed to decrease them. More details on the scenario reduction method can be found in [39]. In SBA model, the Probability Density Function (PDF) curve of the uncertain parameter is divided into several levels with different probabilities. Using PDF, the probability of the uncertain variable in each level can be determined. Stochastic approach is modeled in this paper as a normal Gaussian PDF, where the mean is equal to the forecasted amount. The forecasted amount is mainly considered as the standard deviation of PDF. The formulation of the normal Gaussian PDF is demonstrated as Eqs. (1).

$$f(x|m, \vartheta^2) = \frac{1}{\sqrt{2\pi\vartheta^2}} \exp\left(-\frac{(x-m)^2}{2\vartheta^2}\right), \quad -\infty < x < +\infty \quad (1)$$

where x represents the uncertain parameter, m represents the mean of the forecasted input variable, ϑ^2 and ϑ represent the variance and the standard deviation of the forecasted input variable, respectively. Figure 3 illustrates the normal PDF divided into several segments with different probabilities [40].

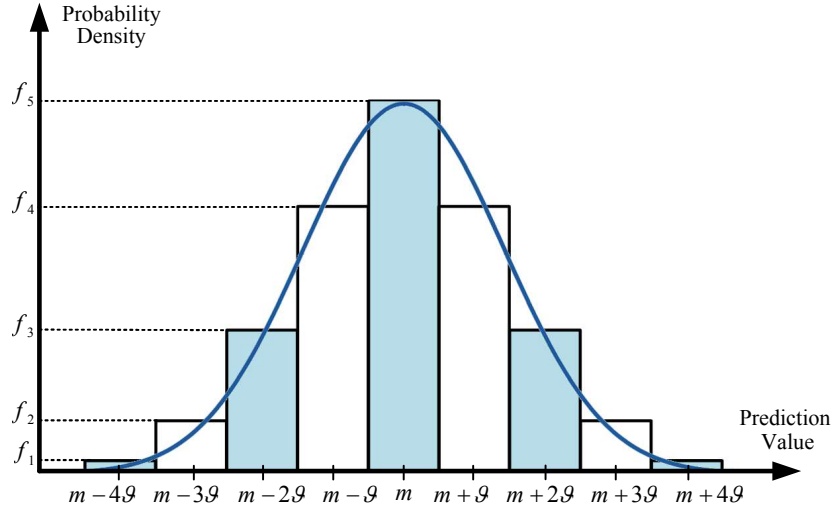


Figure 3: Normal PDF corresponding to the standard deviation of prediction.

2.3. Normal Operation Mode

For the normal operation mode, all MEMGs within the networked structure are assumed to be in the grid-connected mode, i.e., can exchange electrical power with

the upstream grid and can send/receive required power to/from other MEMGs. Optimization procedure in this mode is carried out as follows [41]:

1. Each MEMG is controlled with its local EMS. In the local optimization process, surplus and shortage power in the MEMG is notified to the central EMS at each time-interval.
2. Central EMS performs global optimization. After gathering data from local EMSs and hourly market prices from the utility grid, it runs optimization for minimizing the total operating cost of the networked MEMGs. Central EMS determines the practicality of sharing power among MEMGs and/or exchanging power with the upstream grid.

2.4. Resilience Enhancement Mode

This scheduling mode is considered to enhance the network resilience in contingencies. In case of any extreme event, the physical power connection between the MEMG and the networked system may be lost. The islanded part of the on-fault MEMG that has disconnected from the networked system is taken into account as a new islanded MEMG. Normal-operated grid-connected and on-fault islanded MEMGs can run their local optimization level in different procedures. Figure 4 demonstrates the scheduling stages of resilience enhancement mode. In this mode, problem optimization is conducted in two distinct stages, i.e., (1) resilience enhancement schedule of MEMG and (2) optimization of grid-connected MEMGs. In Stage I (upper section of Figure 4), selection of efficient PEVs is performed for enhancing the resilience of the islanded MEMG in reference to the optimized results of the last time-interval. In Stage II (bottom section of Figure 4), optimization of the grid-connected MEMGs is performed after selecting required PEVs. More details about each stage is described in the following paragraphs.

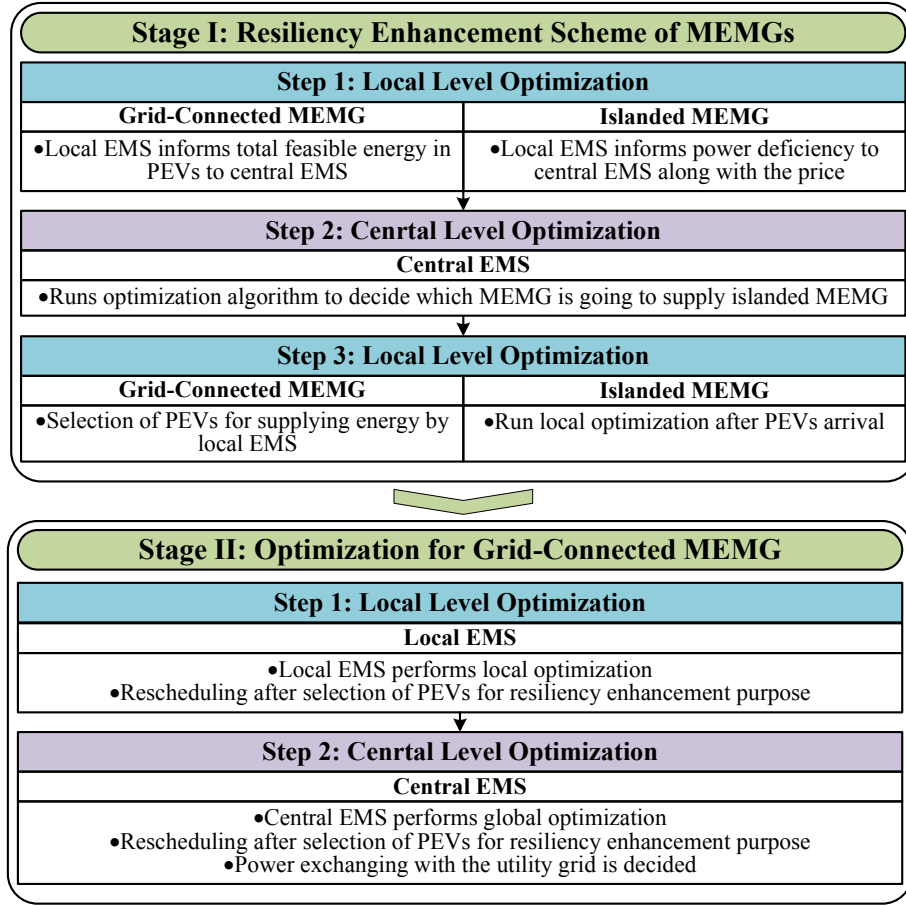


Figure 4: Scheduling stages of resilience enhancement mode

2.4.1. Resilience Enhancement schedule of MEMGs (Stage I)

In this stage, the MEMG agrees to supply power support to the islanded part of the on-fault MEMG via PEVs. In the first step, as illustrated in Figure 4, grid-connected MEMGs notify their total available power support to the central EMS. Here total available power support assigns to the feasible energy in the agreed PEVs among the parked PEVs. Concurrently, islanded MEMG will notify its demanded power support to the central EMS through the intercommunication link. In the second step of Stage I, as illustrated in Figure 4, central EMS runs a global optimization for providing the power support to the islanded MEMG via grid-connected

MEMGs. This resolution is conducted in accordance with the defined distance between MEMGs in the networked structure. The nearest grid-connected MEMG in the proximity of the islanded MEMG supplies the demanded power support through PEVs sent. This procedure will decrease the energy utilization of PEVs while traveling to/from the on-fault MEMG. In the third step of Stage I, the local EMSs of MEMGs decide in reference to the data provided to them by central EMS. Central EMS makes a decision which MEMG will send the power support in step 2, and local EMSs of MEMGs require to opt which PEV should be travelled to supply power support to islanded MEMG. This resolution is vital when the total available power support in the MEMG is more than the requested power deficiency. Accordingly, the minimal amount and the major efficient PEVs are selected among the agreed ones to be sent. By conducting this optimization step, an optimal resolution is performed in selecting the required PEVs for resilience enhancement schedule.

2.4.2. Optimization of the Grid-Connected MEMGs (Stage II)

In Stage I of the resilience enhancement schedule of the networked MEMGs, PEVs are chosen for realizing the required resilience of the islanded MEMG. Thus, there is a necessity for rescheduling the grid-connected MEMGs in the networked system. In the first step of Stage II, the local EMSs of MEMGs run the local optimization as in the normal operation mode for the optimal scheduling of the MEMG. In this step, optimization is carried out by taking into account those PEVs that will depart the MEMG. In this step of optimization, the grid-connected MEMGs share their surplus and shortage power to central EMS. The data related to the surplus/shortage power are assigned for global optimization. While in the second step, based on the data received from local EMSs of grid-connected MEMGs, central EMS runs global optimization. Also, for grid-connected MEMGs, the central EMS will run the similar optimization procedure as in normal operation by redispatching electrical power among MEMGs and/or exchanging with the upstream grid.

3. Formulations of the Proposed Optimization Algorithm

To carry out an optimization algorithm for the MAS-based networked MEMGs, mathematical modelling is formulated. Both normal operation and resilience enhancement modes are designed to minimize the operating cost and enhance the resilience of the system.

3.1. Normal Operation Mode

3.1.1. Local EMS of MEMG

In the hierarchical energy management approach for optimal scheduling of energy resources, the total operating cost of the MEMGs at the local level is minimized. The local level objective function of the proposed stochastic optimization problem of MEMG m is formulated by Eq. (2) ($\forall m \in M_n, t \in T, s \in S$) [9].

$$\min \text{Cost}_m = \sum_t \sum_s \gamma_s \left[\varphi_{m,t,s}^{\text{MT}} + \varphi_{m,t,s}^{\text{CHP}} + \varphi_{m,t,s}^{\text{HES}} + \varphi_{m,t,s}^{\text{BES}} + \varphi_{m,t,s}^{\text{EV}} + \varphi_{m,t,s}^{\text{Short}} - \Re_{m,t,s}^{\text{Sur}} \right] \quad (2)$$

$$\varphi_{m,t,s}^{\text{MT}} = \sum_{G_m} \left[a_g^{\text{MT},1} \cdot p_{g,t,s}^{\text{MT}} + a_g^{\text{MT},2} \cdot \sigma_{g,t,s}^{\text{MT,UC}} \right] \quad (3)$$

$$\varphi_{m,t,s}^{\text{CHP}} = \sum_{C_m} \left[\varphi_{1,c}^{\text{CHP}} \cdot (p_{c,t,s}^{\text{CHP}})^2 + \psi_{1,c}^{\text{CHP}} \cdot (H_{c,t,s}^{\text{CHP}})^2 + \varphi_{2,c}^{\text{CHP}} \cdot p_{c,t,s}^{\text{CHP}} + \psi_{2,c}^{\text{CHP}} \cdot H_{c,t,s}^{\text{CHP}} + \varphi_{3,c}^{\text{CHP}} + \psi_{3,c}^{\text{CHP}} \right] \quad (4)$$

$$\varphi_{m,t,s}^{\text{HES}} = \sum_{H_m} \mu_t^{\text{Hyd,char}} \cdot p_{h,t,s}^{\text{P2H}} \quad (5)$$

$$\varphi_{m,t,s}^{\text{BES}} = \sum_{B_m} \mu_t^{\text{BES}} \cdot \left[\eta^{\text{BES}} \cdot p_{b,t,s}^{\text{BES,ch}} - (1/\eta^{\text{BES,dch}}) \cdot p_{b,t,s}^{\text{BES,dch}} \right] \quad (6)$$

$$\varphi_{m,t,s}^{\text{PEV}} = \sum_{V_m} \mu_t^{\text{PEV}} \cdot \left[\eta^{\text{PEV,ch}} \cdot p_{v,t,s}^{\text{PEV,ch}} - (1/\eta^{\text{PEV,dch}}) \cdot p_{v,t,s}^{\text{PEV,dch}} \right] \quad (7)$$

$$\varphi_{m,t,s}^{\text{Short}} = \mu_t^{\text{GB}} \cdot p_{m,t,s}^{\text{Short}} \cdot \sigma_{m,t,s}^{\text{Short}} \quad (8)$$

$$\Re_{m,t,s}^{\text{Sur}} = \mu_t^{\text{GS}} \cdot p_{m,t,s}^{\text{Sur}} \cdot \sigma_{m,t,s}^{\text{Sur}} \quad (9)$$

In the objective function of the local EMS presented by Eq. (2), the first and second parts are the MEMG operating costs of generated electricity and heat energies in MT and CHP units, respectively. The third and fourth parts indicate costs of charging and discharging power of BESs and PEVs, respectively. The fifth part indicates the charging cost of HESs. The sixth and seventh parts show the MEMG operating cost of buying electrical energy from the utility grid and the revenue gained by selling electrical energy to the utility grid, respectively, as a consequence of market price signals. The cost functions of the energy provided by the MTs, CHP units, BESs, PEVs, and HESs are formulated by Eqs. (3)-(7), respectively. Also, the functions of selling electrical energy to the utility grid and buying electrical energy from the utility grid are represented by Eqs. (8) and (9), respectively.

The problem constraints indicated by Eqs. (10)-(14) ensure that an MT output be within its allowed generation capacity. The MT generation limits are taken into account with commitment states, up/down ramp-rate boundaries, and start-up/shut-down states constraints ($\forall g \in G_m, t \in T, s \in S$) [40].

$$p_g^{MT,min} \cdot \sigma_{g,t,s}^{MT,UC} \leq p_{g,t,s}^{MT} \leq p_g^{MT,max} \cdot \sigma_{g,t,s}^{MT,UC} \quad (10)$$

$$p_{g,t-1,s}^{MT} - p_{g,t,s}^{MT} = p_g^{MT,RU} \cdot [1 - \sigma_{g,t,s}^{SU}] \quad (11)$$

$$p_{g,t,s}^{MT} - p_{g,t-1,s}^{MT} = p_g^{MT,RD} \cdot [1 - \sigma_{g,t,s}^{SD}] \quad (12)$$

$$\sigma_{g,t,s}^{SU} + \sigma_{g,t,s}^{SD} < 1 \quad (13)$$

$$\sigma_{g,t,s}^{SU} - \sigma_{g,t,s}^{SD} - \sigma_{g,t,s}^{UC} + \sigma_{g,t-1,s}^{UC} = 0 \quad (14)$$

The operation region of CHP units is designated in a linear formulation as Eqs. (15)-(19) ($\forall c \in C_m, t \in T, s \in S$) [9]. Eq. (15) shows the operation region under the line AB. Beside, the upper operation region of line BC and line CD are described by Eqs. (16) and (17), respectively. Also, the upper boundary of heat and power generations of the CHP unit are presented by Eqs. (18) and (19), respectively.

$$\frac{PA_c^{CHP} - PB_c^{CHP}}{HA_c^{CHP} - HB_c^{CHP}} \cdot [H_{c,t,s}^{CHP} - HA_c^{CHP}] - p_{c,t,s}^{CHP} + PA_c^{CHP} \geq 0 \quad (15)$$

$$\begin{aligned} & \frac{PB_c^{CHP} - PC_c^{CHP}}{HB_c^{CHP} - HC_c^{CHP}} \cdot [H_{c,t,s}^{CHP} - HB_c^{CHP}] \\ & - p_{c,t,s}^{CHP} + PB_c^{CHP} \leq (1 - \sigma_{c,t,s}^{CHP,UC}) Z \end{aligned} \quad (16)$$

$$\frac{PC_c^{CHP} - PD_c^{CHP}}{HC_c^{CHP} - HD_c^{CHP}} [H_{c,t,s}^{CHP} - HC_c^{CHP}] - P_{c,t,s}^{CHP} + PC_c^{CHP} \leq (1 - \sigma_{c,t,s}^{CHP,UC}) Z \quad (17)$$

$$0 \leq H_{c,t,s}^{CHP} \leq HB_c^{CHP} \cdot \sigma_{c,t,s}^{CHP,UC} \quad (18)$$

$$0 \leq P_{c,t,s}^{CHP} \leq PA_c^{CHP} \cdot \sigma_{c,t,s}^{CHP,UC} \quad (19)$$

The CHP unit constraints of ramp-up, ramp-down, minimum down-time, and minimum up-time are also given by by Eqs. (20)-(26) ($\forall c \in C_m, t \in T, s \in S$) [9].

$$P_{c,t,s}^{CHP} - P_{c,t-1,s}^{CHP} \leq P_c^{CHP,RU} (1 - \sigma_{c,t,s}^{CHP,SU}) + P_c^{CHP,min} \cdot \sigma_{c,t,s}^{CHP,SU} \quad (20)$$

$$P_{c,t-1,s}^{CHP} - P_{c,t,s}^{CHP} \leq P_c^{CHP,RD} (1 - \sigma_{c,t,s}^{CHP,SD}) + P_c^{CHP,min} \cdot \sigma_{c,t,s}^{CHP,SD} \quad (21)$$

$$\sum_{h=1}^{t+UT_j^{CHP}-1} \sigma_{j,h,s}^{CHP,UC} \geq UT_j^{CHP} \cdot \sigma_{c,t,s}^{CHP,SU} \quad (22)$$

$$\sum_{h=1}^{t+DT_j^{CHP}-1} (1 - \sigma_{j,h,s}^{CHP,UC}) \geq DT_j^{CHP} \cdot \sigma_{c,t,s}^{CHP,SD} \quad (23)$$

$$\sigma_{c,t+1,s}^{CHP,UC} - \sigma_{c,t,s}^{CHP,UC} \leq \sigma_{c,t+1,s}^{CHP,SU} \quad (24)$$

$$\sigma_{c,t,s}^{CHP,UC} - \sigma_{c,t+1,s}^{CHP,UC} \leq \sigma_{c,t+1,s}^{CHP,SD} \quad (25)$$

$$\sigma_{c,t+1,s}^{CHP,UC} - \sigma_{c,t,s}^{CHP,UC} \leq \sigma_{c,t+1,s}^{CHP,SU} - \sigma_{c,t+1,s}^{CHP,SD} \quad (26)$$

Eqs. (27)-(31) show the constraints of HESs ($\forall h \in H_m, t \in T, s \in S$) [9]. The level of hydrogen energy stored at time t is described by Eq. (27) and limited by Eq. (28) based on the storage system potential. Eq. (29) guarantees that the value of power converted to hydrogen be within its allowed capacity limits. Furthermore, Eq. (30) bounds the amount of converted hydrogen to power. Plus, Eq. (31) shows that the power cannot be converted to hydrogen and stored hydrogen cannot be converted to power, simultaneously.

$$E_{h,t,s}^{HES} = E_{h,t-1,s}^{HES} + \eta^{P2H} \cdot P_{h,t,s}^{P2H} - (1/\eta^{H2P}) P_{h,t,s}^{H2P} - P_{h,t,s}^{Hyd,ind} \quad (27)$$

$$E_h^{HES,min} \leq E_{h,t,s}^{HES} \leq E_h^{HES,max} \quad (28)$$

$$P_h^{P2H,min} \cdot \sigma_{h,t,s}^{P2H} \leq P_{h,t,s}^{P2H} \leq P_h^{P2H,max} \cdot \sigma_{h,t,s}^{P2H} \quad (29)$$

$$P_{(h)}^{H2P,min} \cdot \sigma_{h,t,s}^{H2P} \leq P_{h,t,s}^{H2P} \leq P_{(h)}^{H2P,max} \cdot \sigma_{h,t,s}^{H2P} \quad (30)$$

$$\sigma_{h,t,s}^{P2H} + \sigma_{h,t,s}^{H2P} \leq 1 \quad (31)$$

The BES constraints of charging, discharging, and SoC are demonstrated in Eqs. (32)-(36), respectively ($\forall b \in B_m, t \in T, s \in S$) [2]. The BES is considered as the power demand at the charging time-interval and as the energy generator at the discharging time-interval.

$$SOC_{b,t,s}^{BES} = SOC_{b,t-1,s}^{BES} + \left(p_{b,t,s}^{BES,ch} \cdot \eta^{BES,ch} - p_{b,t,s}^{BES,dch} / \eta^{BES,dch} \right) / p_b^{BES,cap} \quad (32)$$

$$SOC_b^{BES,min} \leq SOC_{b,t,s}^{BES} \leq SOC_b^{BES,max} \quad (33)$$

$$0 \leq p_{b,t,s}^{BES,ch} \leq p_b^{BES,cap} \cdot \sigma_{b,t,s}^{BES,ch} \cdot (1 - SOC_{b,t-1,s}^{BES}) / \eta^{BES,ch} \quad (34)$$

$$0 \leq p_{b,t,s}^{BES,dch} \leq p_b^{BES,cap} \cdot \sigma_{b,t,s}^{BES,dch} \cdot SOC_{b,t-1,s}^{BES} \cdot \eta^{BES,dch} \quad (35)$$

$$\sigma_{b,t,s}^{BES,ch} + \sigma_{b,t,s}^{BES,dch} \leq 1 \quad (36)$$

The PEV constraints are indicated by Eqs. (37)-(43) ($\forall v \in V_m, t \in [t_v^{arr}, t_v^{dep}]$, $s \in S$) [9]. The PEV energy balance is formulated by Eq. (37). Eqs. (38)-(40) show the upper/lower limits of PEV charging/discharging. Eq. (41) guarantees that each PEV be in its allowed capacity and SoC. Eq. (42) is the resilience constraint that ensures the store energy in the parked PEVs for resilience purpose based on the constraint presented in [42]. Besides, each PEV should be charged to its targeted SoC at the time of departure as represented by Eq. (43).

$$SOC_{v,t,s}^{PEV} = SOC_{v,t-1,s}^{PEV} + \left(p_{v,t,s}^{PEV,ch} \cdot \eta^{PEV,ch} - p_{v,t,s}^{PEV,dch} / \eta^{PEV,dch} \right) / p_v^{PEV,cap} \quad (37)$$

$$0 \leq p_{v,t,s}^{PEV,ch} \leq p_v^{PEV,cap} \cdot \sigma_{v,t,s}^{PEV,ch} \cdot (1 - SOC_{v,t-1,s}^{PEV}) / \eta^{PEV,ch} \quad (38)$$

$$0 \leq p_{v,t,s}^{PEV,dch} \leq p_v^{PEV,cap} \cdot \sigma_{v,t,s}^{PEV,dch} \cdot SOC_{v,t-1,s}^{PEV} \cdot \eta^{PEV,dch} \quad (39)$$

$$\sigma_{v,t,s}^{PEV,ch} + \sigma_{v,t,s}^{PEV,dch} \leq 1 \quad (40)$$

$$SOC_v^{PEV,min} \leq SOC_{v,t,s}^{PEV} \leq SOC_v^{PEV,max} \quad (41)$$

$$SOC_v^{PEV,min} + E_v^{PEV,res} \leq SOC_{v,t,s}^{PEV} \quad (42)$$

$$SOC_{v,t^{dep},s}^{PEV} = SOC_v^{PEV,dep} \quad (43)$$

The shortage and the surplus power of MEMG m are constrained by Eqs. (44) and (45) ($\forall m \in M_n, t \in T, s \in S$) [40].

$$\sigma_{m,t,s}^{\text{Short}} \cdot p_{m,t,s}^{\text{Short}} + \sigma_{m,t,s}^{\text{Sur}} \cdot p_{m,t,s}^{\text{Sur}} = p_{m,t,s}^{\text{Ex}} \quad (44)$$

$$\sigma_{m,t,s}^{\text{Short}} + \sigma_{m,t,s}^{\text{Sur}} \leq 1 \quad (45)$$

In order to realize a resilient hierarchical energy management of MEMGs, the power/heat balance constraint between the total generation and consumption in each MEMG is vital. Therefore, the power/heat balance constraints at MEMG m at hour t for scenario s are presented by Eqs. (46) and (47), respectively ($\forall m \in M_n, t \in T, s \in S$) [9].

$$\begin{aligned} \sum_{I_m} p_{i,t,s}^{\text{Load}} &= p_{m,t,s}^{\text{Short}} - p_{m,t,s}^{\text{Sur}} + \sum_{G_m} p_{g,t,s}^{\text{MT}} + \sum_{C_m} p_{c,t,s}^{\text{CHP}} \\ &+ \sum_{E_m} [p_{e,t,s}^{\text{WT}} + p_{e,t,s}^{\text{PV}}] + \sum_{H_m} [p_{h,t,s}^{\text{H2P}} - p_{h,t,s}^{\text{P2H}}] \\ &+ \sum_{B_m} [p_{b,t,s}^{\text{BES,dch}} - p_{b,t,s}^{\text{BES,ch}}] + \sum_{V_m} [p_{v,t,s}^{\text{PEV,dch}} - p_{v,t,s}^{\text{PEV,ch}}] \end{aligned} \quad (46)$$

$$\sum_{I_m} H_{i,t,s}^{\text{Load}} = \sum_{C_m} H_{c,t,s}^{\text{CHP}} \quad (47)$$

3.1.2. Central EMS of the networked MEMGs

Eq. (48)-(52) shows the central EMS optimization of the networked MEMGs ($\forall m \in M_n, \forall n \in N_n, t \in T, s \in S$) [43]. The primary objective of the central EMS is to run global optimization to minimize the total operating cost of the networked MEMGs, based on the data collected from the local EMSs of the MEMGs regarding the surplus/shortage power at the local optimization level. The first part in the objective function of Eq. (48) indicates the cost of buying electricity from the utility grid, and the second part indicates the profit of selling electricity to the utility grid.

$$\min \sum_m \sum_t \sum_s [\mu_t^{\text{GB}} \cdot p_{m,t,s}^{\text{GB}} - \mu_t^{\text{GS}} \cdot p_{m,t,s}^{\text{GS}}] \quad (48)$$

Internal power exchange from one MEMG to another MEMG is described by Eq. (49). It is clear from Eq. (49) that the total power sent from M MEMGs must be equal to the total power received by N MEMGs in the networked system. Eq. (50) shows that the total power sent and sold by any MEMG m at the time t must be equal

to the surplus power of the MEMG. The amount of power received by MEMG m from any other MEMG and power acquired from the utility grid at time t is shown by Eq. (51). Besides, total surplus power in the system is proportionally redispatched among MEMGs with power shortages based on Eq. (52).

$$\sum_{m=1}^M \sum_{n=1}^N \sum_t p_{m \rightarrow n, t, s}^{\text{Send}} = \sum_{m=1}^M \sum_{n=1}^N \sum_t p_{m \leftarrow n, t, s}^{\text{Rec}}; \quad \forall n \neq m \quad (49)$$

$$\sum_{n=1}^N p_{m \rightarrow n, t, s}^{\text{Send}} + p_{m, t, s}^{\text{GS}} = p_{m, t, s}^{\text{Sur}}; \quad \forall n \neq m \quad (50)$$

$$\sum_{n=1}^N p_{m \leftarrow n, t, s}^{\text{Rec}} + p_{m, t, s}^{\text{GB}} = p_{m, t, s}^{\text{Short}}; \quad \forall n \neq m \quad (51)$$

$$\sum_{n=1}^N p_{m \leftarrow n, t, s}^{\text{Rec}} = \frac{p_{m, t, s}^{\text{Short}}}{\sum_m p_{m, t, s}^{\text{Short}}} \cdot \sum_m p_{m, t, s}^{\text{Sur}}; \quad \forall n \neq m \quad (52)$$

3.2. Proposed Resilience Enhancement Mode

An optimization algorithm has been proposed in this mode to supply energy support to the on-fault islanded MEMG. Therefore, the energy support is supplied to the on-fault islanded MEMG from normal-operated grid-connected MEMGs via PEVs to realize further resilience. The energy support is the energy requested by the on-fault islanded MEMG after applying its maximum local energy resources, including MTs, CHP units, RESs, HESSs, BESSs, and parked PEVs.

3.2.1. Resilience Enhancement schedule of MEMGs (Stage I)

In Stage I of this scheduling mode, the normal-operated grid-connected MEMGs have already conducted the local optimization in the preceding time-interval based on Eqs. (2)-(47). Local EMSs of MEMGs provide the optimized results to the energy stored in the PEVs' battery. The parked PEVs parked are involved in the resilience enhancement schedule. For PEVs that supply energy and participate in the resilience enhancement schedule, their total stored energy is notified to the central EMS. Eq. (53) indicates the objective function of the islanded MEMGs ($\forall m \in M_f, t \in [t_f, T], s \in S$). The first and second parts of Eq. (53) show the MTs and the CHP units generation costs, respectively, and the third part shows the price

for buying power from the networked system to compensate the power deficiency. The on-fault islanded MEMG notifies its requested power to central EMS along with the buying price of that power at each time-interval during the extreme events.

$$\min \varphi_{m,t,s}^{MT} + \varphi_{m,t,s}^{CHP} + \varphi_{m,t,s}^{Short} \quad (53)$$

MT, CHP-unit, HES, BES, and PEVs constraints are the same as given in Eqs. (10)-(14), Eqs. (15)-(26), Eqs. (27)-(31), Eqs. (32)-(36), and Eqs. (37)-(43). Besides, the heat balance constraint is similar to Eq. (47). Power deficiency, RES power generation, MT and CHP unit power generation, BES discharging energy, amount of H2P from HESs, and discharging energy of parked PEVs should be balanced by the total electricity consumption, BES charging energy, amount of P2H from HESs, and charging energy of parked PEV at each time-interval, as illustrated by Eq. (54) ($\forall m \in M_f, t \in [t_f, T], s \in S$) [9].

$$\begin{aligned} \sum_{I_m} p_{i,t,s}^{Load} = & p_{m,t,s}^{Short} + \sum_{G_m} p_{g,t,s}^{MT} + \sum_{C_m} p_{c,t,s}^{CHP} \\ & + \sum_{E_m} [p_{e,t,s}^{WT} + p_{e,t,s}^{PV}] + \sum_{H_m} [p_{h,t,s}^{H2P} - p_{h,t,s}^{P2H}] \\ & + \sum_{B_m} [p_{b,t,s}^{BES,dch} - p_{b,t,s}^{BES,ch}] + \sum_{V_m} [p_{v,t,s}^{PEV,dch} - p_{v,t,s}^{PEV,ch}] \end{aligned} \quad (54)$$

In Stage II, the objective of central EMS is to globally optimize the energy supplied to the on-fault islanded MEMG. Central EMS performs the optimization after collecting data from the local EMSs of MEMGs in Stage I. Eq. (55) is the objective function ($\forall m \in M_f, t \in [t_f, T], s \in S$), in which the data of the distance between the MEMGs and the value of energy required to be supplied by normal-operated grid-connected MEMGs to the on-fault islanded MEMG are assigned. Eq. (56) represents the data of the distance between the MEMGs. If the on-fault islanded MEMGs be further than one and available energy support be less than the total requested energy, the required energy is proportionally dispatched among the MEMGs.

$$\max \sum_{m=1}^M \sum_{n=1}^N E_{m \rightarrow n,t,s}^{PEV,sup} \cdot J_{m \rightarrow n}^{Dis} \quad (55)$$

$$J_{m \rightarrow n}^{Dis} = 1 - (D_{m \rightarrow n} / D_{m \rightarrow n}^{max}); \quad \forall J \neq [0, 1] \quad (56)$$

Eq. (57) shows that normal-operated grid-connected MEMGs can provide energy support less than or equal to available energy stored in the parked PEVs. $E_{m \rightarrow n, t, s}^{\text{Available}}$ indicates the total energy stored in PEVs of MEMG m that has conformed to send energy support to the on-fault islanded MEMG n . Eqs. (58) and (59) show the relation of the energy available and participation level of PEV owners. Eq. (60) indicates that the total energy supplied by 'm' normal-operated MEMGs must be less than or equal to the amount of power deficiency in 'n' on-fault islanded MEMGs. The power deficiency in the on-fault islanded MEMGs is defined by Eq. (61) [2]. $P_{m, t, s}^{\text{Def}} \geq 0$ indicates that the maximum applied power generation in the on-fault islanded MEMGs is lower than the remaining connected loads. In such a condition, the power support is demanded from the normal-operated grid-connected MEMGs. $P_{m, t, s}^{\text{Def}} \leq 0$ indicates that the maximum applied power generation is greater than the remaining connected loads. This condition is not considered as the resilience enhancement mode, hence, no power support is demanded from other MEMGs.

$$E_{m \rightarrow n, t, s}^{\text{PEVsup}} \leq E_{m \rightarrow n, t, s}^{\text{Available}} \quad (57)$$

$$E_{m \rightarrow n, t, s}^{\text{Available}} = \omega_{m, t, s}^{\text{Agree}} \cdot E_{m, t, s}^{\text{PEV, parked}} \quad (58)$$

$$\omega_{m, t, s}^{\text{Agree}} = \sum_{V_m} v_{v, t, s}^{\text{Agree}} / N_{m, t, s}^{\text{EV, parked}} \quad (59)$$

$$\sum_{n=1}^N E_{m \rightarrow n, t, s}^{\text{PEVsup}} \leq P_{n, t, s}^{\text{def}}; \quad \forall n \neq m \quad (60)$$

$$P_{m, t, s}^{\text{def}} = \sum_{m \in M_f} \left[\sum_{I'_m} P_{i, t, s}^{\text{Load}} - \sum_{G'_m} P_{g, t, s}^{\text{MT, max}} - \sum_{C'_m} P_{c, t, s}^{\text{CHP}} - \sum_{E'_m} [P_{e, t, s}^{\text{WT}} + P_{e, t, s}^{\text{PV}}] \right. \\ \left. - \sum_{H'_m} P_{h, t, s}^{\text{H2P, max}} - \sum_{B'_m} P_{b, t, s}^{\text{BES, dch, max}} - \sum_{V'_m} P_{v, t, s}^{\text{PEV, dch}} \right] \quad (61)$$

The third and final objective of this stage is to select the minimum and most efficient PEVs after receiving data from central EMS, as illustrated in Eq. (62) ($\forall v \in V_m, t \in [t_{fs}, t_{fe}], s \in S$).

$$\min \sum_{v=1}^V v_{v, t, s}^{\text{Agree}} \cdot E_f^{\text{PEV}} \quad (62)$$

Eq. (62) is subjected to the constraints given in Eqs. (63)-(65) ($\forall v \in V_m, t \in [t_{fs}, t_{fe}], s \in S$). A PEV is able to supply energy support less than or equal to the stored energy of its battery, as described in Eq. (63). The departure of PEVs to supply energy support to the islanded MEMG is controlled by Eq. (64). $v_{v,t,s}^{\text{Agree}}$ indicates the participation status of the PEV owner, i.e., 1 for PEV that wants to supply energy and 0 otherwise. Eq. (65) shows the constraint of energy balance, in which PEVs supply energy support equal to the amount of energy deficiency requested by the on-fault islanded MEMG.

$$E_{v,t,s}^{\text{PEV,sup}} \leq E_{v,t,s}^{\text{PEV,store}} \quad (63)$$

$$v_{v,t,s}^{\text{Agree}} = \begin{cases} 1, & \text{if } E_{v,t,s}^{\text{PEV,sup}} \neq 0 \\ 0, & \text{otherwise} \end{cases} \quad (64)$$

$$\sum_v E_{v,t,s}^{\text{PEV,sup}} = P_{n,t,s}^{\text{def}} - P_{n,t,s}^{\text{Shed}}, \quad \forall n \in N_n \quad (65)$$

3.2.2. Optimization of the Grid-Connected Microgrids (Stage II)

After achieving the optimal resolution for the resilience enhancement mode, the normal-operated grid-connected MEMGs reschedule the local resources at local and global optimization levels. It has been decided which PEVs will depart MEMGs for resilience enhancement schedule. The local resources are rescheduled at the local optimization level by taking into account the parked PEVs only. The optimization of this level is similar to the MEMG optimization in the normal operation mode demonstrated by Eqs. (2)-(47), where time $t \in [t_c, T]$. After collecting the data of surplus/shortage power, the central EMS runs global optimization for internal/external power exchanging as in normal operation mode, which is demonstrated in Eq. (48), subjected to Eqs. (49)-(52), where time $t \in [t_c, T]$.

The flowchart shown in Figure 5 summarizes the proposed hierarchical stochastic EMS for the MAS-based networked MEMGs for both normal operation and resilience enhancement modes. In the proposed EMS, before checking the operating mode, the input parameters are defined. Then, the uncertain scenarios for renewable units, power/heat loads, and parking time of PEVs are generated applying SBA

method and the number of generated scenarios is also reduced to desired scenarios using a scenario reduction method. For the normal operation mode, first, the local optimization is carried out by local EMSs of MEMGs ($M = 4$). Then, the global optimization is carried out by the central EMS. During extreme events, the local EMSs of MEMGs optimize the normal-operated grid-connected and the on-fault islanded MEMGs. Therefore, the shortage/surplus power and the requested power support by the on-fault islanded MEMGs are informed to the central EMS. The number of the normal-operated grid-connected MEMGs (M_N) and the on-fault islanded (M_F) MEMGs are regularly updated during the optimization procedure. Hence, the central EMS decides which MEMG will supply power support to the on-fault islanded MEMGs and update the local EMSs of MEMGs. The local EMS selects the efficient PEVs for supplying the requested energy support. Ultimately, the grid-connected MEMGs ($M = M_N$) are rescheduled when the fault still exists. After resolving the fault, the optimization is carried out once again for all MEMGs ($M = M_N + M_F$).

3.2.3. Formulation of Resilience Enhancement Factor

In this section, a resilience enhancement factor is formulated for investigating the enhancement in the resilience of the on-fault islanded MEMG through the utilization of the parked PEVs. The resilience of the on-fault islanded MEMG is directly calculated by applying the load survived with and without PEVs of the on-fault islanded MEMG as represented by Eq. (66). It can be mentioned that the load survived without PEVs is the exact energy supplied to survive load with local available power resources in the on-fault islanded MEMG, while the load survived with PEVs is the total load survived with PEVs and local energy resources.

$$\text{Resilience Enhancement Factor} = \left[1 - \frac{\text{Load Survived without PEVs}}{\text{Load Survived with PEVs}} \right] \times 100 \quad (66)$$

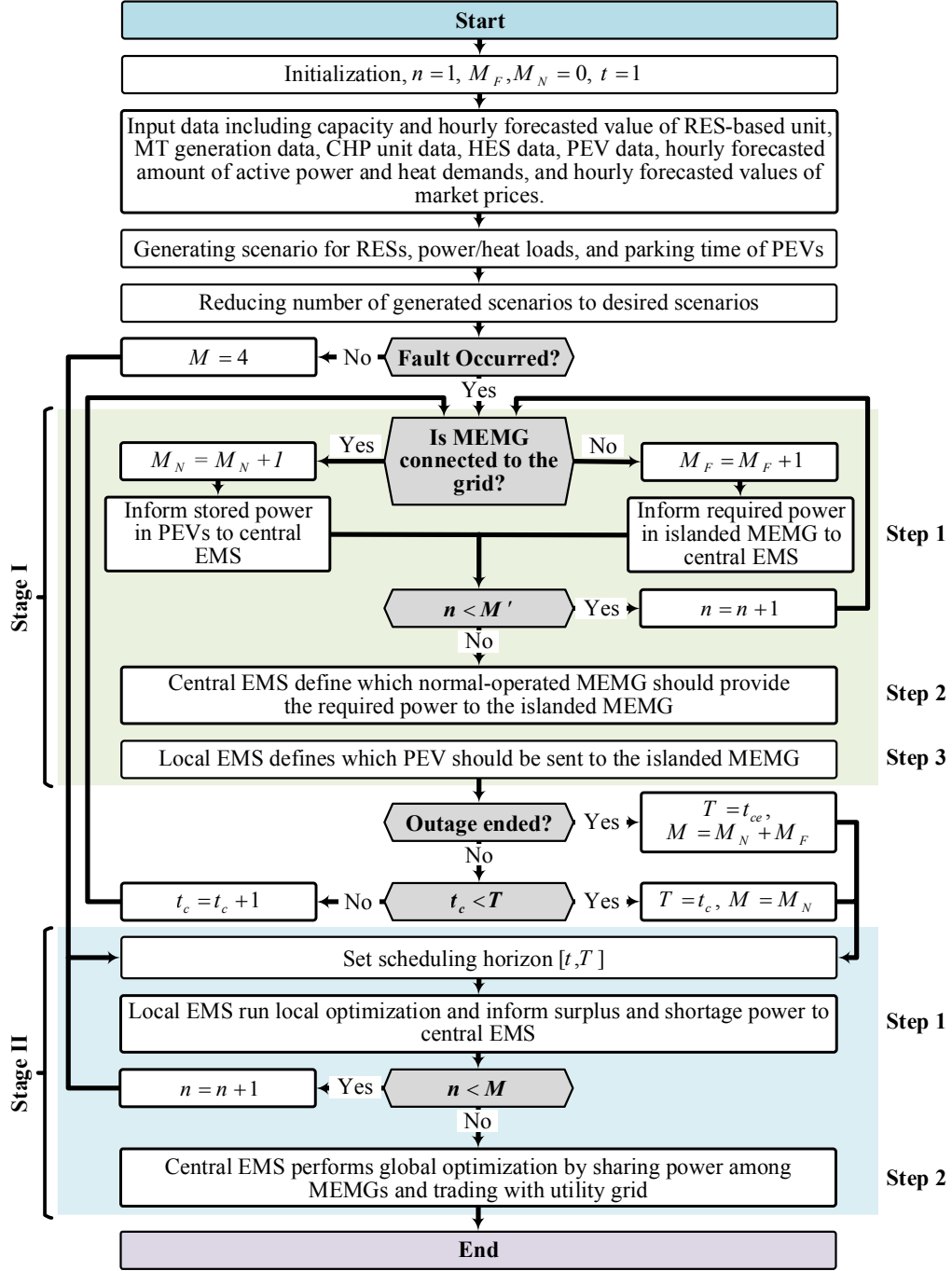


Figure 5: Flowchart for proposed hierarchical EMS of MAS-based networked MEMG system

4. Numerical Simulation

As illustrated in Figure 6, the derived optimization strategy is modeled in a MAS with four networked MEMGs to minimize the total operating cost of each MEMG over a 24-hour time-interval scheduling. Each MEMG contains dispatchable DGs including CHP units and MTs, non-dispatchable DGs including PVs and WTs, multi-ESSs including BESs and HESs, PEVs as MESSs, and electrical and heat demands. Table 2 shows the installed capacity of RESs. Table 3 shows the location and technical/economic details of MTs. The CHP units' information and their feasible operation regions are also demonstrated in Tables 4 and 5, respectively. The location and details of HESs and BESs are shown in Tables 6 and 7, respectively. Table 8 shows the capacities and efficiencies (energy consumption per km) of PEVs. Arrival/Departure timing details of parked PEVs in MEMGs are given in Figure 7. The hourly forecasted multipliers of electrical loads, heat demands, and renewable units are illustrated in Figure 8. Furthermore, the time-of-use signals of market prices are represented in Figure 9. The maximum electrical and heat loads of each node in the networked system are presumed to be 100 kW and 30 kW, respectively. The distance between the physical common bus and MEMGs are 3 km, 5 km, 8 km, and 12 km for MEMG1, MEMG2, MEMG3, and MEMG4, respectively. $p_{MT,min}$ is set to be zero for all MTs. Charging/Discharging efficiency of PEVs is set to be 95% and targeted SoC is set to the maximum capacity of PEVs. The initial SoC of PEVs is selected between 25% to 35% of the battery capacities at random. Charging/Discharging efficiency of BESs is set to be 95%. Also, P2H and H2P efficiencies are set to be 80% and 70%, respectively. μ_t^{BES} , $\mu_t^{Hyd, Char}$, and μ_t^{PEV} are assumed to be 0.004 \$/kWh, 0.002 \$/kWh, and 0.03 \$/kWh, respectively.

The proposed networked MEMGs can be scheduled in normal operation and resilience enhancement modes. Initially, the networked system is operated in the normal operation mode. In case of any extreme event, the scheduling can be switched into the resilience enhancement mode. In normal operation mode, the optimization results of local EMSs of MEMGs and central EMS are simulated for a 24-hour time-interval. In order to analyze the efficiency of the resilience enhancement sched-

ule, two faulty case studies (CS) are defined under diverse conditions. In CS1 of the resilience enhancement schedule, it is supposed that a fault exists in the connection line between node 10 and node 11 in MEMG1 at hour 17. Accordingly, the line 10–11 is disconnected and the MEMG1 is segregated into two zones. The grid-connected zone of MEMG1 is assumed as MEMG1-1 and the islanded zone of MEMG1 is assumed as MEMG1-2. After two hours, the fault is resolved. Therefore, the scheduling of the networked MEMGs is switched into the resilience enhancement mode for hours 17 and 18. It should be mentioned that in CS1, the MEMG1-1 is assumed as a grid-connected normal-operated MEMG, while the MEMG1-2 is assumed as an on-fault islanded MEMG based on the existing power deficiency in MEMG1-2. In CS2, it is supposed that together with the existed fault in line 10–11 of MEMG1, another fault exists in the tie-line with the common physical bus, simultaneously. Accordingly, the MEMG1 segregated into two on-fault islanded MEMG1-1 and MEMG1-2. This case is designed to challenge the proposed resilience enhancement strategy in a further extreme event.

When PEVs are not parked in the PLs or disagree to supply energy support, the energy stored in BESs, HESs, and dispatchable DGs are employed to supply required energy to the on-fault MEMG. The stochastic hierarchical EMS for the proposed model is solved using CPLEX solver under the GAMS 24.8.3 environment. It is worth noting that all above-mentioned assumption are not constrained to the adjusted amounts and can alter subject to any CS.

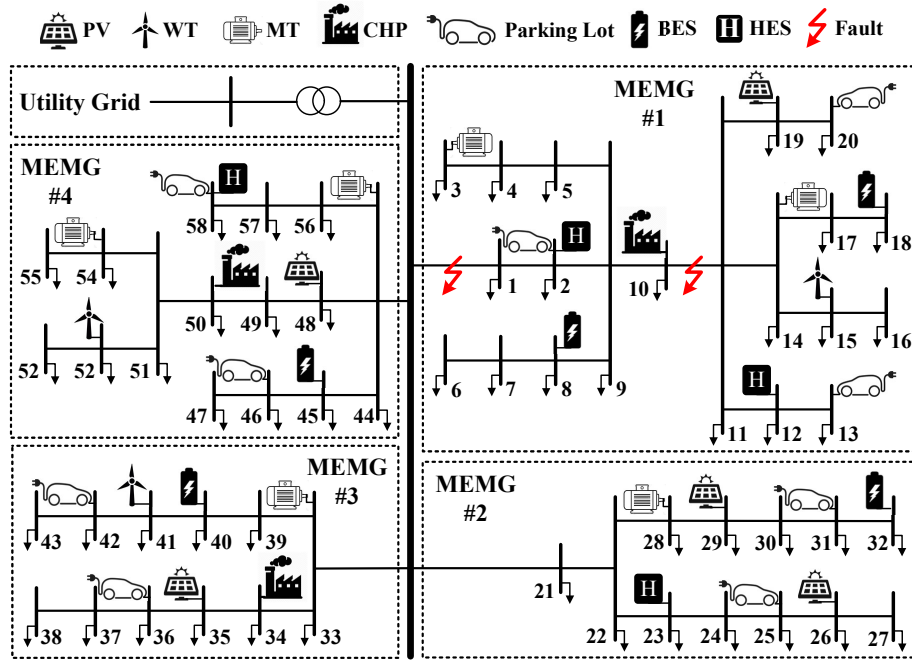


Figure 6: Test system with four MAS-based networked MEMGs

Table 2: Installed capacity and location of RESs

MEMG #	Location	Type	Capacity (kW)
MEMG 1	Node 15	WT	150
	Node 19	PV	100
MEMG 2	Node 26	PV	200
	Node 29	PV	150
MEMG 3	Node 35	PV	100
	Node 41	WT	150
MEMG 4	Node 48	WT	200
	Node 52	PV	150

Table 3: Location and technical/economic details of MTs

MEMG #	Location	$\alpha^{MT,1}$ (\$/MW)	$\alpha^{MT,2}$ (\$/MW)	$P^{MT,max}$ (kW)	$P^{MT,RU}$ (kW)	$P^{MT,RD}$ (kW)
MEMG 1	Node 02	13.325	19.96	400	300	200
	Node 06	12.349	13.98	300	150	150
MEMG 2	Node 19	26.802	31.02	700	350	350
MEMG 3	Node 33	10.784	32.93	400	200	200
MEMG 4	Node 44	17.922	10.03	450	225	225
	Node 54	12.974	10.05	350	175	175

Table 4: Location and details of CHP units

MEMG #	Location	$\phi^{CHP,1}$	$\phi^{CHP,2}$	$\phi^{CHP,3}$	$\psi^{CHP,1}$	$\psi^{CHP,2}$	$\psi^{CHP,3}$	$P^{CHP,RU}$	$P^{CHP,RD}$	U^{CHP}	D^{CHP}
MEMG 1	Node 10	0.0350	36.0	12.5	0.027	1.6	0.011	214	214	3	3
MEMG3	Node 34	0.0435	14.5	26.5	0.030	4.2	0.031	247	247	3	3
MEMG4	Node 50	0.038	25	17	0.019	3.7	0.039	302	302	3	3

Table 5: Feasible operation regions of CHP units (kW/kWth)

MEMG #	Location	PA^{CHP}	PB^{CHP}	PC^{CHP}	PD^{CHP}	HA^{CHP}	HB^{CHP}	HC^{CHP}	HD^{CHP}
MEMG1	Node 10	214	187	68	75	0	264	127	0
MEMG3	Node 34	494	430	162	198	0	360	209	0
MEMG4	Node 50	302	264	96	106	0	373	180	0






Table 6: Location and details of HESs (kW)

MEMG #	Location	$P^{P2H,max}$	$P^{P2H,min}$	$P^{H2P,max}$	$P^{H2P,min}$	$E^{HES,max}$	$E^{HES,min}$
MEMG1	Node 02	60	20	60	20	120	25
	Node 12	50	15	50	15	100	20
MEMG2	Node 23	90	30	90	30	180	35
MEMG4	Node 58	70	25	70	25	140	30

Table 7: Location and details of BESs (kW)

MEMG #	Location	$p^{BES, cap}$	$p^{BES, ch, max} / p^{BES, dch, max}$
MEMG1	Node 08	200	100
	Node 18	150	75
MEMG2	Node 32	150	75
MEMG3	Node 40	300	150
MEMG4	Node 45	200	100

Table 8: Battery capacities and availability of parked PEVs

Model of PEV	Battery Cap. (kW)	Energy Eff. (W/km)	PEV Number			
			MEMG1	MEMG2	MEMG3	MEMG4
	50	150	1,2, 11,12, 21,22	1,2, 9,10, 17,18	1,2, 7,8	1,9
	40	160	3,4, 13,14, 23,24	3,4, 11,12, 19,20	3,4, 9,10	2,3, 10,11
	65	230	5,6, 15,16, 25	-	-	4,12
	85	220	7,8, 17,18	5,6, 13,14	5,6, 11,12	5,13
	40	170	9,10, 19,20	7,8, 15,16	-	6,7, 8,14, 15,16

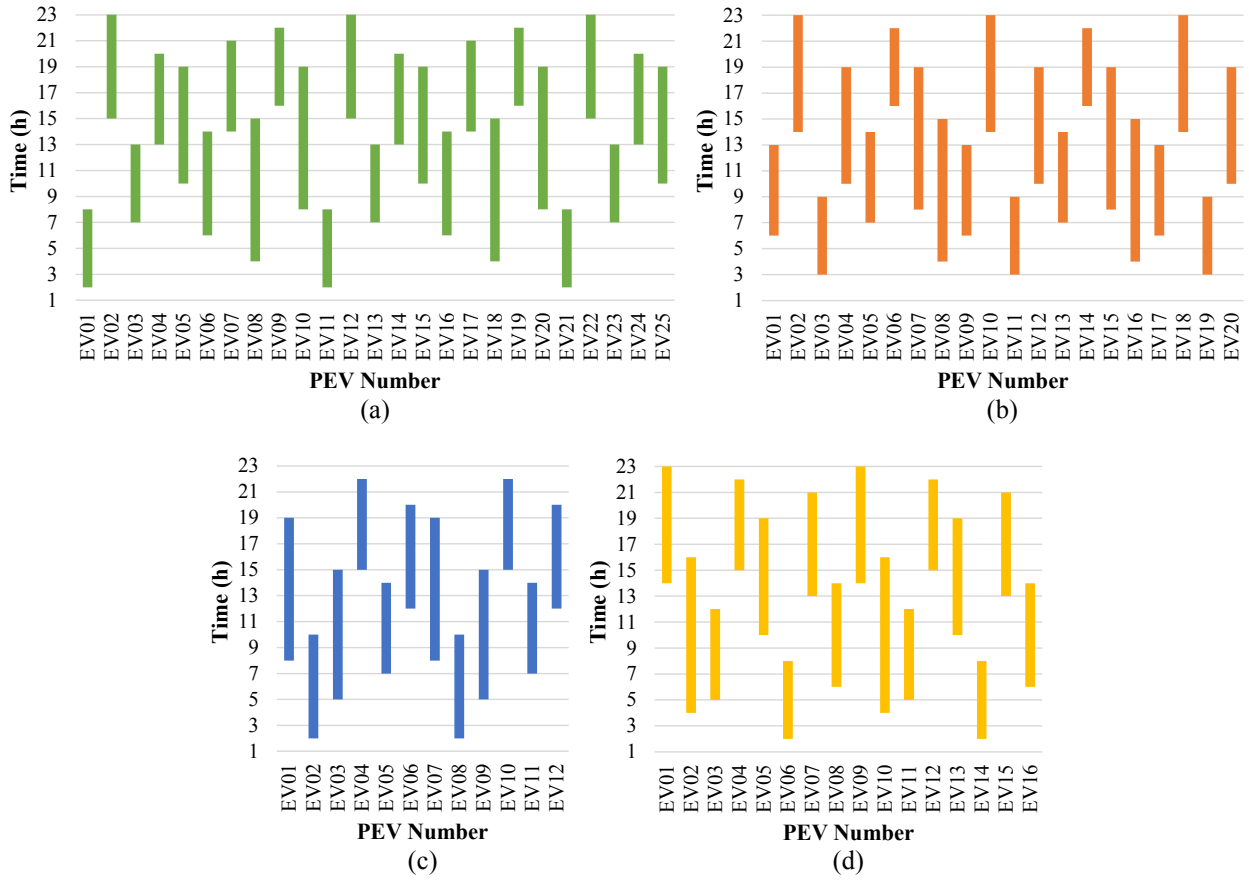


Figure 7: Arrival/Departure timing of PEVs in (a) MEMG1, (b) MEMG2, (c) MEMG3, and (d) MEMG4

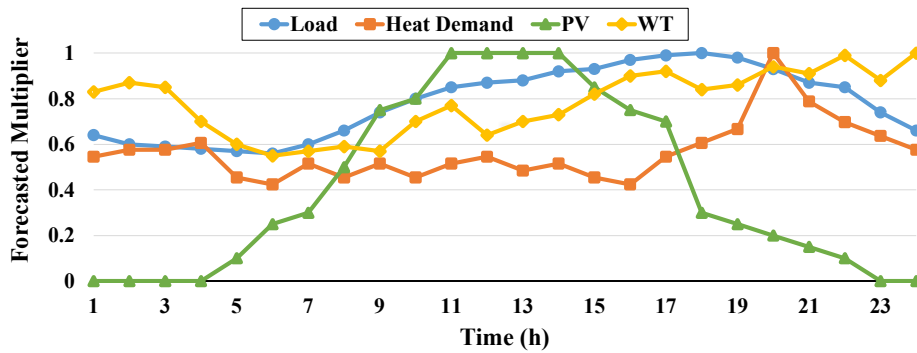


Figure 8: Hourly forecasted multipliers of electrical load, heat demands, and RESs



Figure 9: Time-of-use signals of market prices

4.1. Results of Normal Operation Mode

In this section, the optimized results of local EMSs of MEMGs and central EMS is analysed in normal operation mode. During this mode, the networked MEMGs work as usual and the MEMGs can exchange electrical power with the upstream grid. Figures 10-13 show the results of the power balance in MEMG1, MEMG2, MEMG3, and MEMG4, respectively, at each time-interval t in normal operation mode. It can be observed from Figure 10 that MTs and CHP units being the cheaper source in MEMG1, generate power throughout the day. Also, RESs, including WTs and PVs, provide low-cost energy throughout the day. Figure 11 shows that MT in MEMG2 operates at its maximum generation capacity during the day. Here, the RESs are PVs; therefore, they generate power only during the daytime. As illustrated in Figure 12, MT in MEMG3 is the most expensive generator among the dispatchable DGs, hence, it generates power only in higher price time-intervals. Also, CHP units and RESs generate power throughout the day. It is clear from Figure 13 that MTs and CHP units in MEMG1 are generating power throughout the day and by RESs.

It can be seen from Figures 10-13 that BESs and HESs are primarily charged in lower price time-intervals and discharged in higher price time-intervals. On the PEVs' arrival time to the PLs, PEV owners prefer to charge their vehicles to the targeted SoC based on the market price behavior. However, few PEVs are charged during peak-load time-intervals to store their targeted SoC in the batteries for resilience objectives; given that batteries of PEVs give less energy stored than the

energy required for resilience objectives on the arrival time. PEVs that arrived before hour 12 are charged when they are parked in the PLs. The remaining PEVs are charged when the market price is lessened again before departure of PEVs. Furthermore, the PEVs that arrive in the off-peak time-intervals (e.g., in the early morning) and depart in the off-peak time-intervals (e.g., in the late evening), discharge energy during peak-load time-intervals. When the electricity consumption is higher than the maximum capacity of power generation, the shortage power is either purchased from the upstream grid or received from neighbouring MEMGs, therefore, the central EMS makes the decision of this procedure.

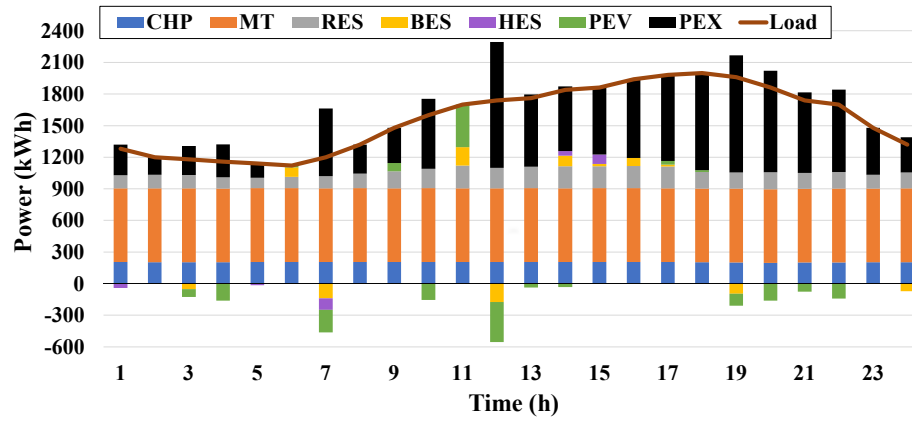


Figure 10: Power balance of MEMG1 in normal operation mode

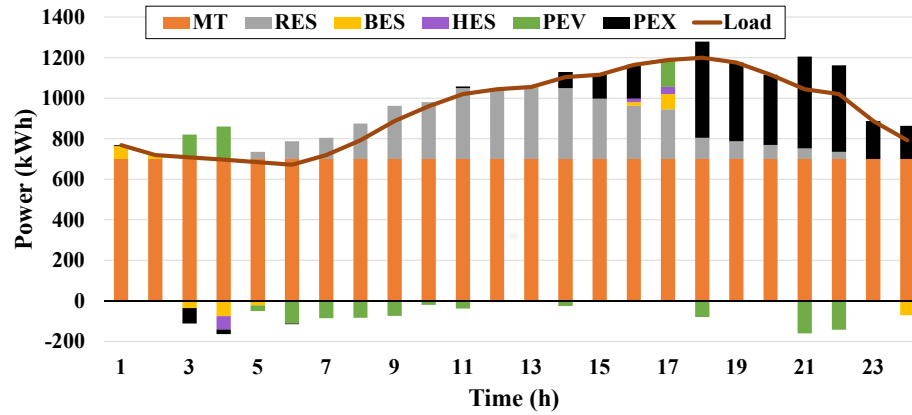


Figure 11: Power balance of MEMG2 in normal operation mode

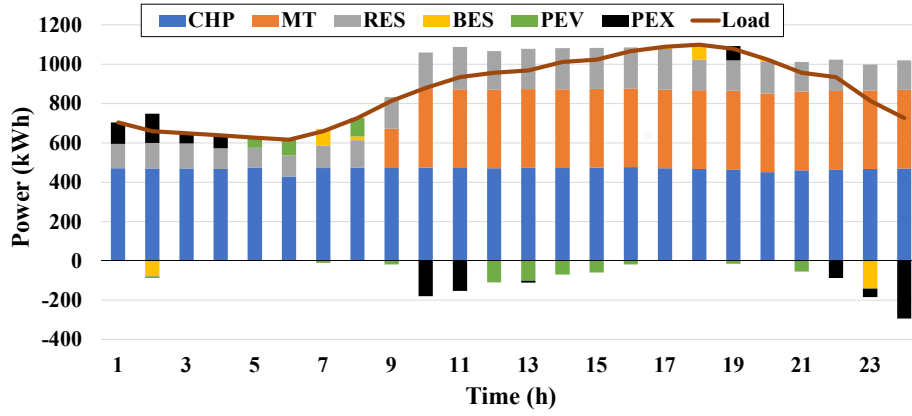


Figure 12: Power balance of MEMG3 in normal operation mode

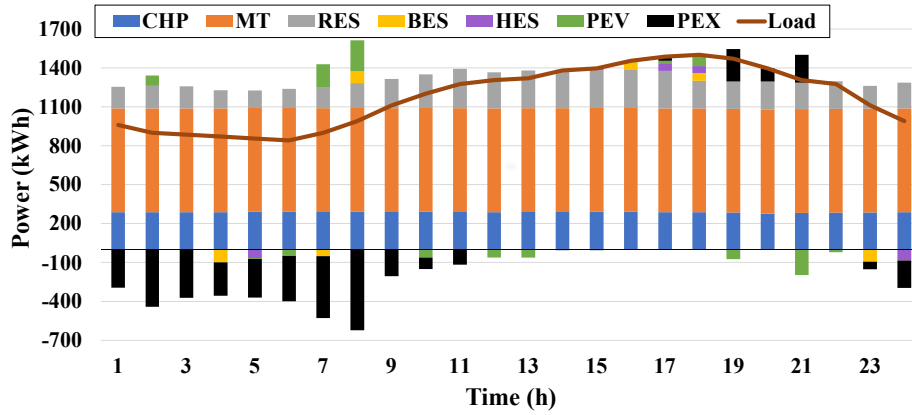


Figure 13: Power balance of MEMG4 in normal operation mode

Central EMS collects the surplus/shortage power data from each MEMG. Then, it either decides to exchange power among MEMGs or with the upstream grid. As shown in Figure 14, MEMG1, MEMG2, and MEMG3 have surplus power shared proportionally in the networked system during the normal operation mode. After internal power exchanging, the remaining surplus/shortage power is traded with the upstream grid. Furthermore, the heat balance of networked MEMGs in normal operation mode is shown in Figure 15. After this stage, the networked MEMG system is now globally optimal.

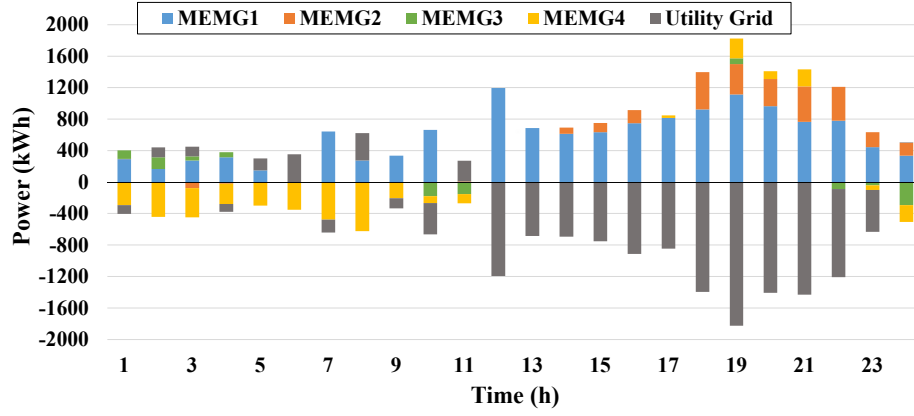


Figure 14: Internal power exchange among MEMGs and external power trading of networked MEMGs with the utility grid in normal operation mode

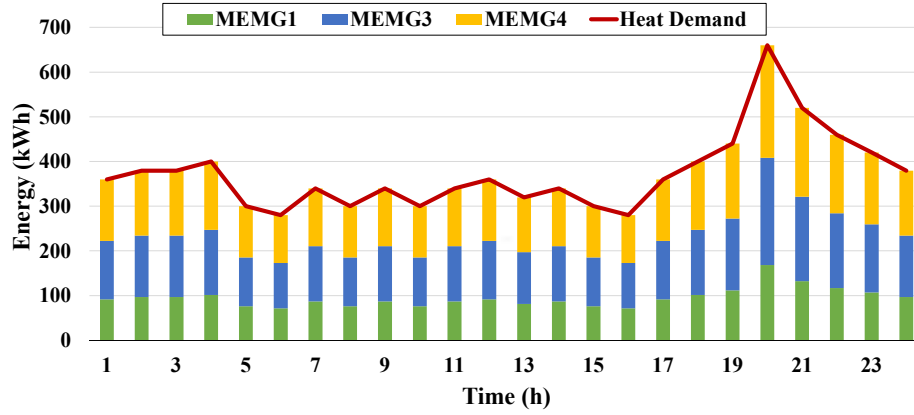


Figure 15: Heat balance of networked MEMGs in normal operation mode

4.2. Results of Resilience Enhancement Mode

Table 9 shows the detailed output values of energy resources and the corresponding power deficiencies received by the central EMS from the on-fault islanded MEMG1-1 for CS1 and on-fault islanded MEMG1-1 and MEMG1-2 for CS2 at hours 17 and 18. It can be seen from Table 9 that MTs generate power at hours 17 and 18 within their maximum allowed generation limits for both CS1 and CS2. Also, CHP units and RESs generate scheduled and forecasted power, respectively, at hours 17 and 18 for both CSs. It should also be mentioned that the CHP unit is not located

at the on-fault islanded MEMG1-1, and no power is generated from this unit for CS1, while the CHP unit located at node 10 generates power in on-fault islanded MEMG1-2 for CS2. Besides, the multi-ESSs, including BESs, HES, and PEVs discharge their maximum available power at hour 17, while the multi-ESSs are empty at hour 18, and there is no available energy to discharge. On the other hand, the forecasted electrical load at hour 18 is higher than at hour 17. Accordingly, the value of power deficiency in MEMG1 for both CSs at 18 is higher than hour 17 and require more energy support from other MEMGs.

Table 9: Detailed output values of energy resources and power deficiency at hours 17 and 18 for CS1 and CS2

Fault Scenario	CS1		CS2	
Time (h)	17	18	17	18
Max CHP Unit Power Output (kW)	0	0	204.62	203.62
Max MT Power Output (kW)	300	300	700	700
RESs Power Output (kW)	208	156	208	156
Max BES Discharge (kW)	18.36	0	18.36	0
Max H2P Energy (kW)	67.5	0	202.5	0
Max PEV Discharge (kW)	112.5	0	301.5	0
Total Power Demand (kW)	990	1000	1980	2000
Power Deficiency (kW)	283.64	544	345.02	940.38

Figure 16 illustrates the total power stored in the parked PEVs of each MEMG during the 24-hour scheduling time horizon. Based on the Eq. (55) and the assumed distance between the physical common bus and MEMGs, the normal-operated MEMG2, MEMG3, and MEMG4 send the power support via available power stored in parked PEVs of the on-fault MEMG1 in order of priority.

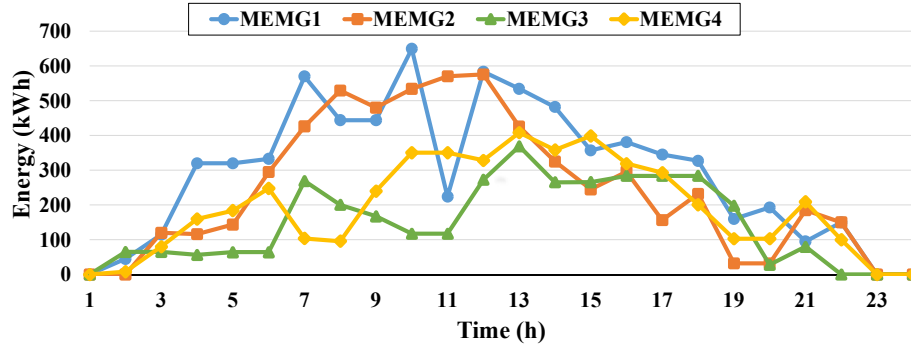


Figure 16: Total power stored in parked PEVs of each MEMG

Figures 17-19 demonstrate the rescheduling results of the local EMS optimization for MEMG2, MEMG3, and MEMG4, respectively, for CS1 and CS2. It can be seen from Figures 17 and 18 that the rescheduling results in CS1 are the same as in CS2 for MEMG2 and MEMG3, since these MEMGs are sending the maximum available energy stored in their whole PEVs to the on-fault MEMG1. For CS1, five out of eight available PEVs in MEMG4 (PEV 1,4,9,13,15) at hour 18 will supply energy to the on-fault MEMG1 while all parked PEVs are sending the available energy stored at hour 18 for CS2. Accordingly, as shown in Figure 19, the rescheduling results are different for CS1 and CS2 for MEMG4. After rescheduling of local EMSs, central EMS receives the data for the global optimization of the networked MEMG system.

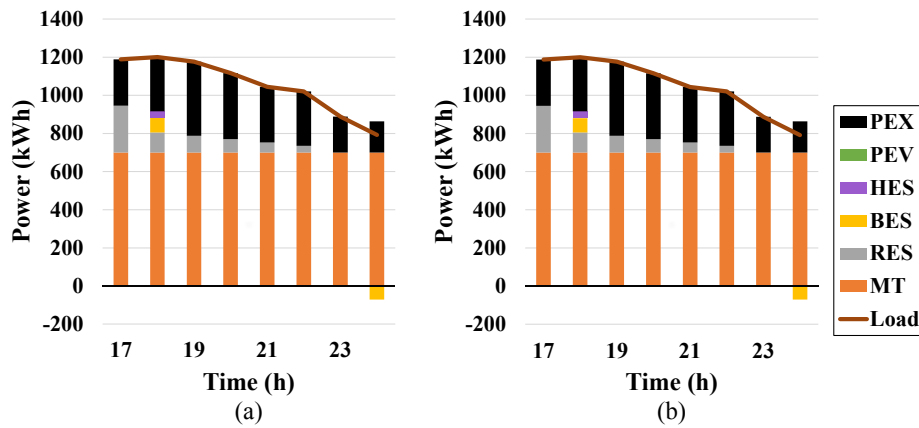


Figure 17: Rescheduling results of MEMG2 for (a) CS1 and (b) CS2

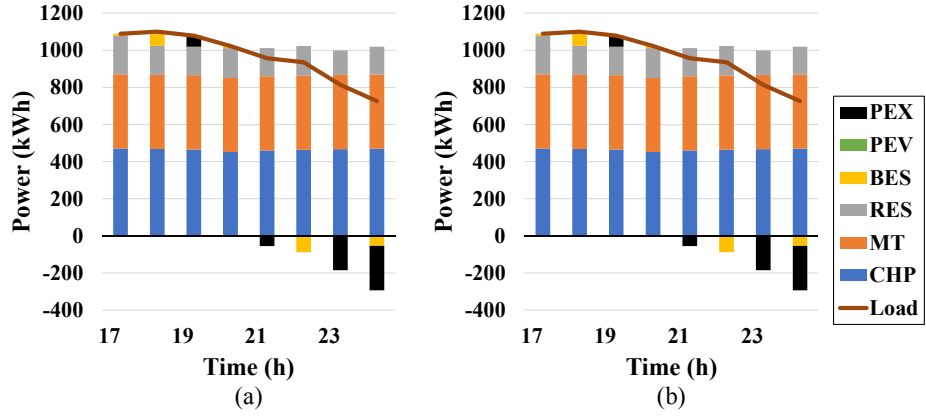


Figure 18: Rescheduling results of MEMG3 for (a) CS1 and (b) CS2

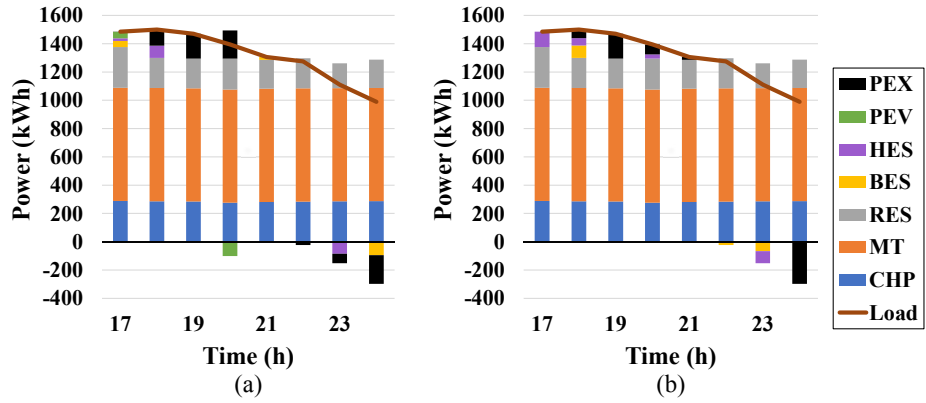


Figure 19: Rescheduling results of MEMG4 for (a) CS1 and (b) CS2

Table 10 shows the exact values of power deficiency and load shedding with diverse participation factors of PEVs for both CSs. It can be seen from Table 10 that grid-connected MEMG1-1 can only supply the available amount of energy at hour 17 for CS1, while this MEMG has power deficiency in CS2 and cannot send any PEVs for power support. For example, MEMG1-1 being next to the MEMG1-2 delivers all possible energy support via its PEVs (equal to 189 kWh) at hour 17 for CS1. The remaining energy support (equal to 94.64 kWh) is delivered through parked PEVs of MEMG2 being closer to MEMG1-2. Besides, if the participation of PEVs in compensating for power shortages is low, the amount of energy supply via parked PEVs

is low. Hence, the possibility of load shedding increases. Using the proposed strategy, a considerable enhancement in the resilience of the on-fault MEMG is obtained altering from 41.6% in CS1 to 21.1% in CS2 for 100% participation.

Table 10: Power deficiency and load shedding values with participation factors of PEVs for CS1 and CS2

$\omega^{\text{Agree}} [0,1]$	Faulty CS #	Time (h)	Energy Supply via Parked PEVs (kW)				p^{Shed} (kW)
			MEMG1-1	MEMG2	MEMG3	MEMG4	
1.00	CS1	17	189	94.64	0	0	No
		18	0	149.35	248.85	145.8	No
	CS2	17	-	244	101.02	0	No
		18	-	0	147.83	271	521.55
0.75	CS1	17	141.75	142.89	0	0	No
		18	0	40.02	186.75	203.25	113.98
	CS2	17	-	183	162.02	0	No
		18	-	0	24.73	203.25	712.4
0.50	CS1	17	94.5	122	68.14	0	No
		18	0	0	56.36	135.5	352.14
	CS2	17	-	122	124.5	98.52	No
		18	-	0	0	36.98	903.4
0.25	CS1	17	47.25	61	62.25	67.75	46.39
		18	0	0	0	0	544
	CS2	17	-	61	62.25	67.75	154.02
		18	-	0	0	0	940.38

Furthermore, the 3D Pareto frontier of the proposed resilience enhancement factor with diverse participation factors and the number of parked PEVs for CS1 and CS2 is presented in Figure 20. It can be observed from Figure 20 that the optimal resilience enhancement that can be achieved in each CS is saturated to a certain amount. Hence, increasing the quantity or the participation of PEVs in compensating for the power deficiency does enhancing resilience further. According to Figure 20, the maximum increase in the resilience of the on-fault islanded MEMG for CS1 is 41.6% for participation factor of 100% and number of PEVs equal to the proposed quantity (Figure 20(a)), and for CS2 is 28.5% for participation factor of 100% and number of PEVs equal to the 150% proposed quantity (Figure 20(b)).

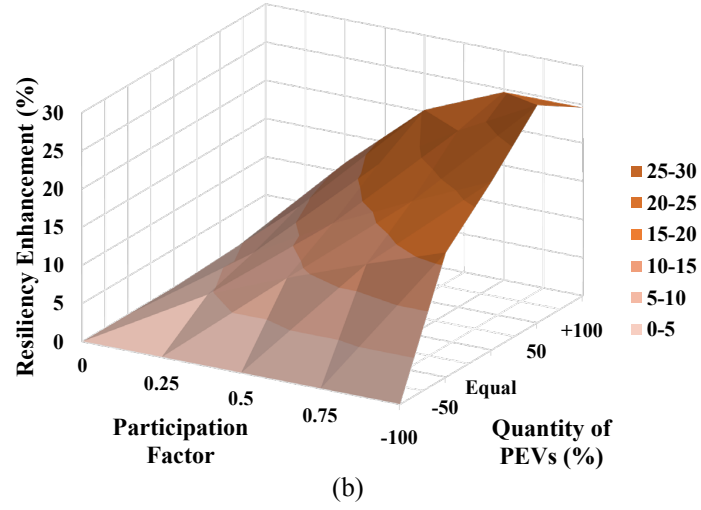
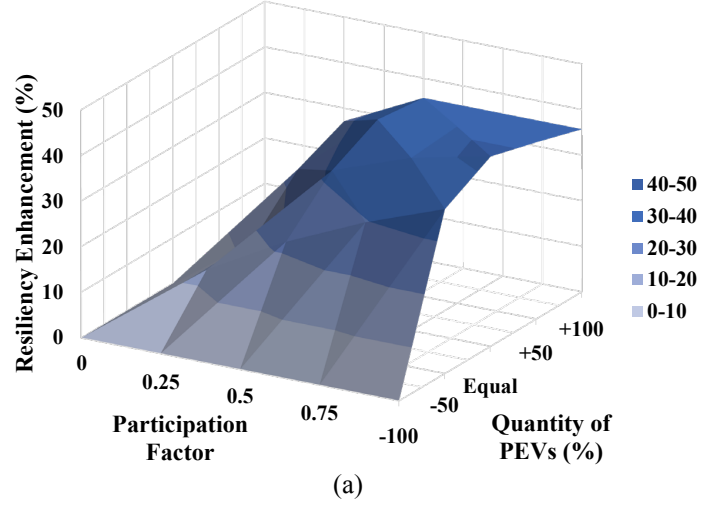


Figure 20: The Pareto frontier of increase in the resilience of on-fault islanded MEMG with participation factor and quantity of PEVs for (a) CS1 and (b) CS2

5. Conclusion

The constraints of ongoing expansion in energy demands, resource depletion, environmental issues, as well as current electricity demand and supply patterns, are insufficient to fulfill the expanding needs of urban areas for ongoing growth. To

address the issues raised above, power energy systems must undergo a revolution. DERs are frequently employed as a useful model for a more affordable and consistent energy supply. This paper introduces a hierarchical stochastic optimization algorithm for the energy management of a MAS with networked MEMGs considering MTs, CHP units, HESs, BESs, and PEVs as MESSs under the uncertainties of RESs, power/heat demand, and arrival/departure timing of PEVs parked in PLs. The MAS framework of the networked MEMGs is optimized applying local EMSs and a central EMS. Each DG and power/heat consumer is controlled by the local EMS of each MEMG, considering the independence of each agent. Accordingly, local EMS is implemented for the local optimization level of MEMGs. After the optimization of energy resources, local EMS of each MEMG sends required data to the central EMS, which is implemented for the global optimization level of the networked MEMGs. Central EMS run the global optimization based on the collected data from the local EMSs.

Initially, the normal operation mode was simulated to illustrate the optimized scheduling of the networked MEMGs without extreme events. In the case of contingencies, the proposed algorithm supplies energy to the on-fault MEMGs from normal-operated grid-connected MEMGs by using PEVs. The procedure of selecting PEVs to supply energy support to the on-fault MEMGs was conducted in three stages. At first, the on-fault islanded and the normal-operated grid-connected MEMGs send the required data of the available energy stored in the parked PEVs to the central EMS. Then, central EMS decides which MEMGs among networked MEMGs will supply energy support to the on-fault islanded MEMG. Finally, the selected MEMGs identify the efficient PEVs to send the requested energy support to the on-fault islanded MEMG. The existing PEVs in the MEMGs can be employed for enhancing the system's resilience, increasing the profit for PEV owners without the necessity of further investment cost for the MEMG operators. The derived model was simulated over a MAS with four networked MEMGs minimizing the total operation cost of each MEMG over a 24-hour operation considering two faulty CSs. The results showed that the proposed algorithm provides energy support to on-fault MEMGs to survive priority loads without any physical tie-line connection among MEMGs.

6. Acknowledgments

This work was supported from DTE Network+ funded by EPSRC grant reference EP/S032053/1.

References

- [1] Y. Wang, C. Chen, J. Wang, R. Baldick, Research on resilience of power systems under natural disasters—a review, *IEEE Transactions on Power Systems* 31 (2) (2016) 1604–1613.
- [2] S. E. Ahmadi, N. Rezaei, H. Khayyam, Energy management system of networked microgrids through optimal reliability-oriented day-ahead self-healing scheduling, *Sustainable Energy, Grids and Networks* 23 (2020) 100387.
- [3] S. E. Ahmadi, N. Rezaei, Reliability-oriented optimal scheduling of self-healing in multi-microgrids, in: *2018 Smart Grid Conference (SGC)*, 2018, pp. 1–6.
- [4] E. Hossain, S. Roy, N. Mohammad, N. Nawar, D. R. Dipta, Metrics and enhancement strategies for grid resilience and reliability during natural disasters, *Applied Energy* 290 (2021) 116709.
- [5] G. Huang, J. Wang, C. Chen, J. Qi, C. Guo, Integration of preventive and emergency responses for power grid resilience enhancement, *IEEE Transactions on Power Systems* 32 (6) (2017) 4451–4463.
- [6] A. Younesi, H. Shayeghi, A. Safari, P. Siano, Assessing the resilience of multi microgrid based widespread power systems against natural disasters using monte carlo simulation, *Energy* 207 (2020) 118220.
- [7] S. E. Ahmadi, N. Rezaei, Distribution network emergency operation in the light of flexibility, in: *Flexibility in Electric Power Distribution Networks*, CRC Press, 2021, pp. 147–174.
- [8] S. Rahgozar, A. Zare Ghaleh Seyyedi, P. Siano, A resilience-oriented planning of energy hub by considering demand response program and energy storage systems, *Journal of Energy Storage* 52 (2022) 104841.

- [9] S. E. Ahmadi, D. Sadeghi, M. Marzband, A. Abusorrah, K. Sedraoui, Decentralized bi-level stochastic optimization approach for multi-agent multi-energy networked micro-grids with multi-energy storage technologies, *Energy* 245 (2022) 123223.
- [10] S. Hosseini, A. Ahmarinejad, M. Tabrizian, M. A. Bidgoli, Resilience enhancement of integrated electricity-gas-heating networks through automatic switching in the presence of energy storage systems, *Journal of Energy Storage* 47 (2022) 103662.
- [11] D. Sadeghi, S. E. Ahmadi, N. Amiri, Satinder, M. Marzband, A. Abusorrah, M. Rawa, Designing, optimizing and comparing distributed generation technologies as a substitute system for reducing life cycle costs, co2 emissions, and power losses in residential buildings, *Energy* (2022) 123947.
- [12] H. Saboori, S. Jadid, Mobile and self-powered battery energy storage system in distribution networks—modeling, operation optimization, and comparison with stationary counterpart, *Journal of Energy Storage* 42 (2021) 103068.
- [13] D. K. Mishra, M. J. Ghadi, L. Li, J. Zhang, M. Hossain, Active distribution system resilience quantification and enhancement through multi-microgrid and mobile energy storage, *Applied Energy* 311 (2022) 118665.
- [14] S. Ghasemi, J. Moshtagh, Distribution system restoration after extreme events considering distributed generators and static energy storage systems with mobile energy storage systems dispatch in transportation systems, *Applied Energy* 310 (2022) 118507.
- [15] S. Zeynali, N. Nasiri, M. Marzband, S. N. Ravadanegh, A hybrid robust-stochastic framework for strategic scheduling of integrated wind farm and plug-in hybrid electric vehicle fleets, *Applied Energy* 300 (2021) 117432.
- [16] S. E. Ahmadi, N. Rezaei, An igdt-based robust optimization model for optimal operational planning of cooperative microgrid clusters: A normal bound-

- ary intersection multi-objective approach, *International Journal of Electrical Power Energy Systems* 127 (2021) 106634.
- [17] K. Yang, C. Li, X. Jing, Z. Zhu, Y. Wang, H. Ma, Y. Zhang, Energy dispatch optimization of islanded multi-microgrids based on symbiotic organisms search and improved multi-agent consensus algorithm, *Energy* 239, Part C (2022) 122105.
 - [18] D. Yu, H. Zhu, W. Han, D. Holburn, Dynamic multi agent-based management and load frequency control of pv/fuel cell/ wind turbine/ chp in autonomous microgrid system, *Energy* 173 (2019) 554–568.
 - [19] M. Elkazaz, M. Sumner, D. Thomas, A hierarchical and decentralized energy management system for peer-to-peer energy trading, *Applied Energy* 291 (2021) 116766.
 - [20] H. r. Gholinejad, J. Adabi, M. Marzband, Hierarchical energy management system for home-energy-hubs considering plug-in electric vehicles, *IEEE Transactions on Industry Applications* (2022) 1–1.
 - [21] J. A. A. Silva, J. C. López, N. B. Arias, M. J. Rider, L. C. da Silva, An optimal stochastic energy management system for resilient microgrids, *Applied Energy* 300 (2021) 117435.
 - [22] S. Nourian, A. Kazemi, Resilience enhancement of active distribution networks in the presence of wind turbines and energy storage systems by considering flexible loads, *Journal of Energy Storage* 48 (2022) 104042.
 - [23] M. Ghasemi, A. Kazemi, E. Bompard, F. Aminifar, A two-stage resilience improvement planning for power distribution systems against hurricanes, *International Journal of Electrical Power Energy Systems* 132 (2021) 107214.
 - [24] H. Wu, Y. Xie, Y. Xu, Q. Wu, C. Yu, J. Sun, Resilient scheduling of messs and rcs for distribution system restoration considering the forced cut-off of wind power, *Energy* 244, Part B (2022) 123081.

- [25] M. A. Gilani, A. Kazemi, M. Ghasemi, Distribution system resilience enhancement by microgrid formation considering distributed energy resources, *Energy* 191 (2020) 116442.
- [26] Q. Sun, Z. Wu, Z. Ma, W. Gu, X.-P. Zhang, Y. Lu, P. Liu, Resilience enhancement strategy for multi-energy systems considering multi-stage recovery process and multi-energy coordination, *Energy* 241 (2022) 122834.
- [27] M. Yan, Y. He, M. Shahidehpour, X. Ai, Z. Li, J. Wen, Coordinated regional-district operation of integrated energy systems for resilience enhancement in natural disasters, *IEEE Transactions on Smart Grid* 10 (5) (2019) 4881–4892.
- [28] B. Taheri, A. Safdarian, M. Moeini-Aghaie, M. Lehtonen, Distribution system resilience enhancement via mobile emergency generators, *IEEE Transactions on Power Delivery* 36 (4) (2021) 2308–2319.
- [29] L. Che, M. Shahidehpour, Adaptive formation of microgrids with mobile emergency resources for critical service restoration in extreme conditions, *IEEE Transactions on Power Systems* 34 (1) (2019) 742–753.
- [30] Z. Li, W. Tang, X. Lian, X. Chen, W. Zhang, T. Qian, A resilience-oriented two-stage recovery method for power distribution system considering transportation network, *International Journal of Electrical Power Energy Systems* 135 (2022) 107497.
- [31] M. Rajabzadeh, M. Kalantar, Improving the resilience of distribution network in coming across seismic damage using mobile battery energy storage system, *Journal of Energy Storage* 52 (2022) 104891.
- [32] J. Kim, Y. Dvorkin, Enhancing distribution system resilience with mobile energy storage and microgrids, *IEEE Transactions on Smart Grid* 10 (5) (2019) 4996–5006.
- [33] M. Nazemi, P. Dehghanian, X. Lu, C. Chen, Uncertainty-aware deployment of mobile energy storage systems for distribution grid resilience, *IEEE Transactions on Smart Grid* 12 (4) (2021) 3200–3214.

- [34] H. Mehrjerdi, S. Mahdavi, R. Hemmati, Resilience maximization through mobile battery storage and diesel dg in integrated electrical and heating networks, *Energy* 237 (2021) 121195.
- [35] B. Kashanizadeh, H. M. Shourkaei, M. Fotuhi-Firuzabad, Short-term resilience-oriented enhancement in smart multiple residential energy system using local electrical storage system, demand side management and mobile generators, *Journal of Energy Storage* 52 (2022) 104825.
- [36] G. Zhang, F. Zhang, X. Zhang, Z. Wang, K. Meng, Z. Y. Dong, Mobile emergency generator planning in resilient distribution systems: A three-stage stochastic model with nonanticipativity constraints, *IEEE Transactions on Smart Grid* 11 (6) (2020) 4847–4859.
- [37] E. A. Javadi, M. Joorabian, H. Barati, A sustainable framework for resilience enhancement of integrated energy systems in the presence of energy storage systems and fast-acting flexible loads, *Journal of Energy Storage* 49 (2022) 104099.
- [38] Y. Wang, A. O. Rousis, G. Strbac, Resilience-driven optimal sizing and pre-positioning of mobile energy storage systems in decentralized networked microgrids, *Applied Energy* 305 (2022) 117921.
- [39] H. Heitsch, W. Römis, Scenario reduction algorithms in stochastic programming, *Scenario Reduction Algorithms in Stochastic Programming* 24 (2) (2003) 187–206.
- [40] S. E. Ahmadi, N. Rezaei, A new isolated renewable based multi microgrid optimal energy management system considering uncertainty and demand response, *International Journal of Electrical Power & Energy Systems* 118 (2020) 105760.
- [41] V.-H. Bui, A. Hussain, H.-M. Kim, A multiagent-based hierarchical energy management strategy for multi-microgrids considering adjustable power and demand response, *IEEE Transactions on Smart Grid* 9 (2) (2018) 1323–1333.

- [42] A. Hussain, V.-H. Bui, H.-M. Kim, A proactive and survivability-constrained operation strategy for enhancing resilience of microgrids using energy storage system, *IEEE Access* 6 (2018) 75495–75507.
- [43] R. Yokoyama, H. Kamada, Y. Shinano, T. Wakui, A hierarchical optimization approach to robust design of energy supply systems based on a mixed-integer linear model, *Energy* 229 (2021) 120343.